
VOLUME 263 · 1 AUGUST 2013 · ISSN 0377-0273
ELSEVIER
Special Issue
Magma System Response to Edifice Collapse
P. Izbekov, E. Gordeev, J. Eichelberger and M. West
(Guest Editors)
M. Rutherford (Editor-in-Chief)
JOURNAL OF
VOLCANOLOGY
AND GEOTHERMAL RESEARCH
AN INTERNATIONAL RESEARCH JOURNAL WITH FOCUS
ON VOLCANIC AND GEOTHERMAL PROCESSES AND
THEIR IMPACT ON THE ENVIRONMENT AND SOCIETY

Journal of Volcanology and Geothermal Research 263 (2013) 3–21

Contents lists available at ScienceDirect

Journal of Volcanology and Geothermal Research

journal homepage: www.elsevier.com/locate/jvolgeores

# Relationship between Kamen Volcano and the Klyuchevskaya group of volcanoes (Kamchatka)

Tatiana G. Churikova [a,c,*], Boris N. Gordeychik [b], Boris V. Ivanov [a], Gerhard Wörner [c]

[a] Institute of Volcanology and Seismology, Far East Branch, Russian Academy of Sciences, 683006 Petropavlovsk-Kamchatskii, Russia
[b] Institute of Experimental Mineralogy, Russian Academy of Sciences, 142432 Chernogolovka, Russia
[c] Geoscience Centre, University of Göttingen, Goldschmidtsrasse 1, 37077 Göttingen, Germany

ARTICLE INFO

*Article history:*
Received 2 February 2012
Accepted 29 January 2013
Available online 9 February 2013

*Keywords:*
Klyuchevskoy Volcano
Bezymianny Volcano
Kamen Volcano
Subduction
Geochemistry
Fractional crystallization

ABSTRACT

Data on the geology, petrography, mineralogy, and geochemistry of rocks from Kamen Volcano (Central Kamchatka Depression) are presented and compared with rocks from the neighbouring active volcanoes. The rocks from Kamen and Ploskie Sopky volcanoes differ systematically in major elemental and mineral compositions and could not have been produced from the same primary melts. The compositional trends of Kamen stratovolcano lavas and dikes are clearly distinct from those of Klyuchevskoy lavas in all major and trace element diagrams as well as in mineral composition. However, lavas of the monogenetic cones on the southwestern slope of Kamen Volcano are similar to the moderately high-Mg basalts from Klyuchevskoy and may have been derived from the same primary melts. This means that the monogenetic cones of Kamen Volcano represent the feeding magma for Klyuchevskoy Volcano. Rocks from Kamen stratovolcano and Bezymianny form a common trend on all major element diagrams, indicating their genetic proximity. This suggests that Bezymianny Volcano inherited the feeding magma system of extinct Kamen Volcano. The observed geochemical diversity of rocks from the Klyuchevskaya group of volcanoes can be explained as the result of both gradual depletion over time of the mantle N-MORB-type source due to the intense previous magmatic events in this area, and the addition of distinct fluids to this mantle source.


## 1. Introduction

The geochemical diversity of volcanic rocks relative to their parent magmas remains one of the most intriguing issues of magma generation in subduction zones. The full measure of this issue is illustrated by the Klyuchevskaya group of volcanoes (KGV) situated in the Central Kamchatka Depression (CKD), which represents one of the most active and productive areas of subduction-related magmatism on the planet. Previous data have shown that the region is characterised by distinct parent magmas ranging from high-Mg and high-Al basalts to high-Mg and calk-alkaline andesites (Khrenov et al., 1991; Churikova, 1993; Kersting and Arculus, 1994; Pineau et al., 1999; Dorendorf et al., 2000; Ozerov, 2000; Mironov et al., 2001; Churikova et al., 2001, 2007; Portnyagin et al., 2007; Turner et al., 2007). Most of these papers, however, only provided data from recently active KGV — Klyuchevskoy, Bezymianny, and Tolbachik. In order to document and understand the full compositional range of magmas, their distribution in space and time, and the genetic relations of KGV magmatism, data on those volcanoes that are not presently active, such as Kamen Volcano and its monogenetic centres, must be evaluated. These older volcanoes should be genetically related to the currently active eruptive centres because they form the basement of the active edifices and should record the past history and evolution of their magma sources.

Kamen Volcano is an extinct system (Fig. 1) located in the central part of the KGV between Klyuchevskoy, Bezymianny, and Ploskie Sopky volcanoes. Kamen Volcano was studied on a reconnaissance basis only in the 1970s. During that time a geological map of this volcano was created and the first petrographic and geochemical data were obtained from its rocks (Ermakov, 1977). One of the largest gravitational Kamchatka collapses in Holocene times was described from the eastern slope of Kamen Volcano (e-Fig. 1) (Melekestsev and Braitseva, 1988; Ponomareva et al., 2006).

Kamen Volcano is close to other active volcanoes and its edifice is large (height 4579.6 m, just 250 m lower than neighbouring Klyuchevskoy Volcano); despite this, modern geochemical studies of Kamen Volcano have not been previously carried out and its relationship and petrogenesis in comparison to other KGV volcanoes are unknown. A modern geochemical study of Kamen Volcano is warranted because it will shed light not only on the history of the volcano itself and its closest neighbours, but also on the history and earlier evolution of the KGV in general. Kamen Volcano, which forms the base of the younger Klyuchevskoy and Bezymianny KGV edifices, is itself

* Corresponding author at: Institute of Volcanology and Seismology, Far East Branch, Russian Academy of Sciences, 683006 Petropavlovsk-Kamchatskii, Russia. Tel.: +79261008373.
*E-mail address:* tchurikova@mail.ru (T.G. Churikova).

0377-0273/$ – see front matter © 2013 Elsevier B.V. All rights reserved.
http://dx.doi.org/10.1016/j.jvolgeores.2013.01.019

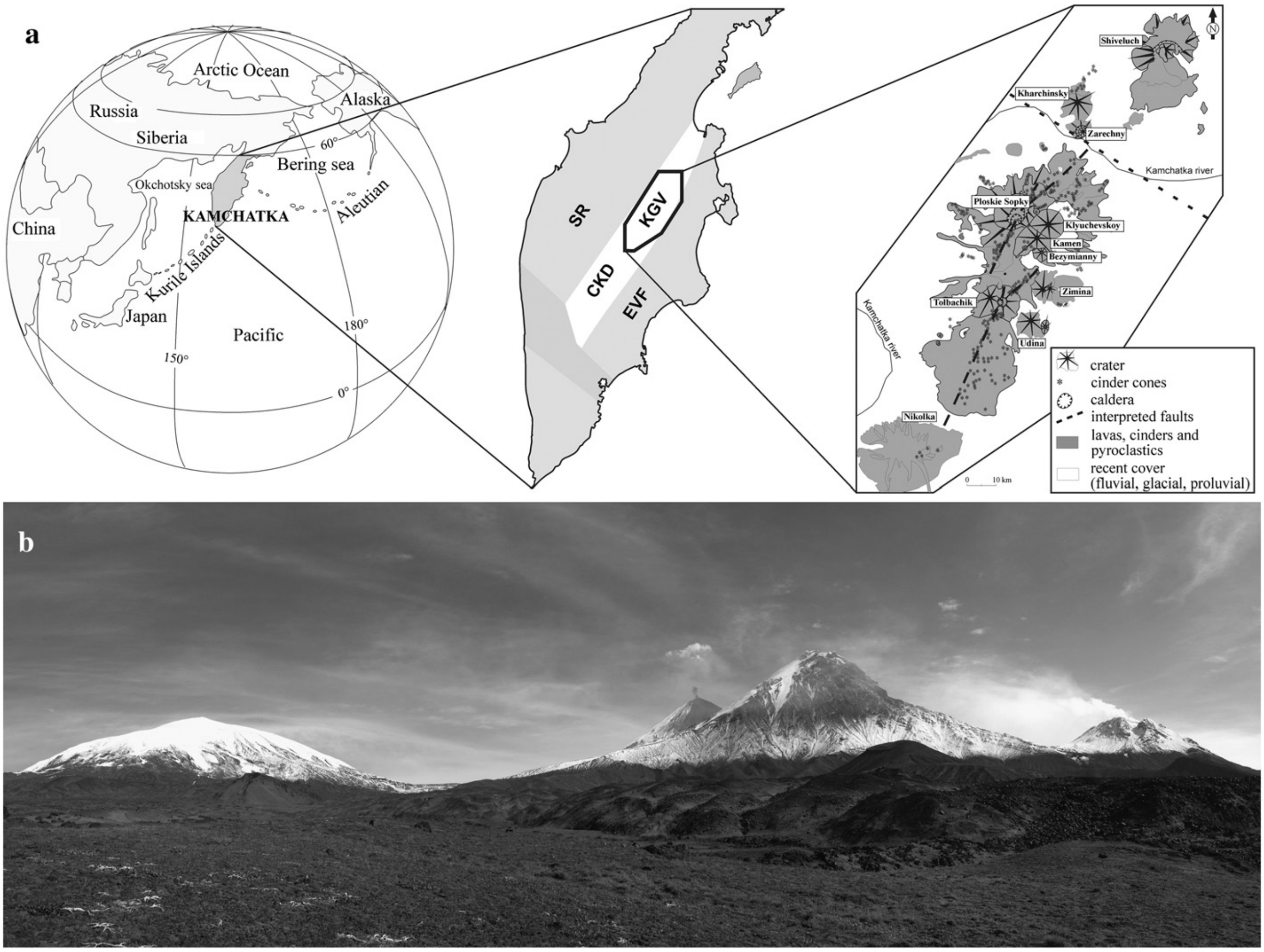


**Fig. 1.** Location map and general view of the studied area: (a) location map of Kamen Volcano. Tectonic sketch of Kamchatka after (Erlich and Gorshkov, 1979) with tree volcanic belts: Eastern Volcanic Front (EVF), Central Kamchatka Depression (CKD), Sredinny Range (SR); map of the Klyuchevskaya group of volcanoes (KGV) after (Melekestsev et al., 1991a); (b) general view of the four neighbouring volcanoes from the Studenaya River valley to the southwest, from left to right: Ploskie Sopky, Klyuchevskoy, Kamen, Bezymianny. Eruptive activity can be seen at Klyuchevskoy Volcano and fumaroles at Bezymianny. Dark hills in the front are the Bogdanovich Glacier covered by glacial debris. Photo taken 31 August 2010.

built on top of a major shield volcano with its centre below Ploskie Sopky Volcano. The distance between the summits of Kamen and Klyuchevskoy is only 5 km, the same as between Kamen and Bezymianny (Fig. 1). Because these volcanic edifices are spatially close, relatively young, and large, the magma production rate of this group is one of the highest for any arc setting worldwide. The close relationship in space and time of the KGV and the common zone of seismicity below them (Tokarev and Zobin, 1970) suggests a common source and a possible genetic relationship between their magmas. However, the lavas of all these neighbouring volcanoes are different: high-Mg and high-Al olivine (Ol)–clinopyroxene (Cpx)–plagioclase (Pl) basalts and basaltic andesites occur at Klyuchevskoy Volcano, and hornblende (Hbl)-bearing andesites and dacites dominate at Bezymianny Volcano. The rocks of Ploskie Sopky Volcano, situated only 10 km NW of Kamen, are represented by medium-high-K subalkaline lavas (Fig. 1). Any attempts to understand the origin of this diversity hinge on this question: What is the geochemical character of lavas from Kamen Volcano, which is situated between these three large active arc volcanoes?

In order to constrain the compositional spectrum of lavas from Kamen stratovolcano, its central dike complex, and the surrounding monogenetic cinder and cinder–lava cones (Fig. 2), we present geological, petrographical, mineralogical, and geochemical data from Kamen Volcano rocks and compare these to its surrounding older and younger centres.

## 2. Geological background

Like other KGV, Kamen Volcano overlies the large lava plateau of a shield volcano (Flerov and Ovsyannikov, 1991; Melekestsev et al., 1991a) with its centre below Ploskie Sopky Volcano. These lavas crop out mainly in the Studenaya and Khapitsa river valleys as well as near the Kozyrevsk and Klyuchi settlements. The age of these plateau lavas was determined by Ar–Ar dating to be 262–274 ka (Calkins, 2004). The edifice of the Kamen stratovolcano formed after the emplacement of the plateau lavas (i.e. since ca. 260 ka) in two stages with different types of eruptions and erupted material. The first stage is characterised by an explosive regime with accumulation of thick pyroclastic deposits composed mainly of tuffs and tuffaceous breccias. The second stage of the stratovolcano was mainly effusive and is represented by thin lava flows that covered the early cone. Numerous dikes – lava flow conduits – also formed during this second stage. A similar sequence was suggested for the formation of Klyuchevskoy (Khrenov et al., 1991) and Stariy Shiveluch

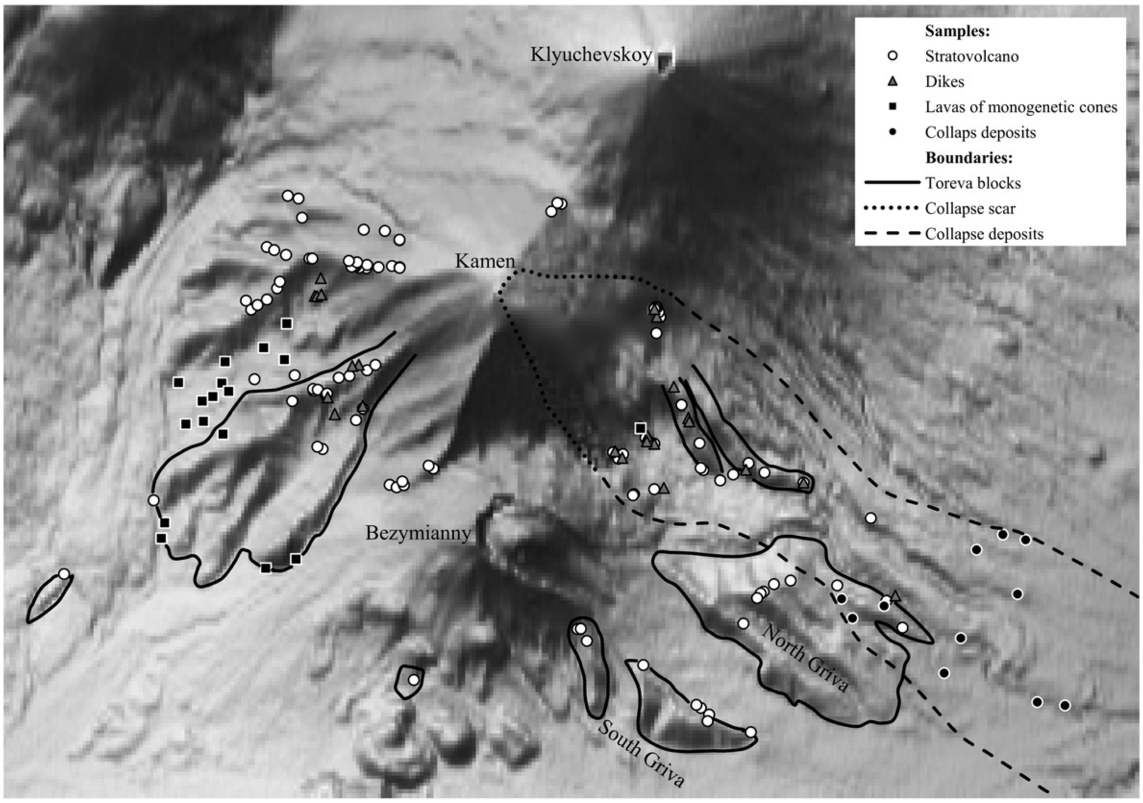


**Fig. 2.** Digital Elevation Model (DEM) map of Kamen Volcano and surrounding (Klyuchevskoy, Bezymianny, Ploskie Sopky) volcanoes and locations of rock samples. The collapse scars and related debris flows from Kamen Volcano are indicated according to the map (Ermakov, 1977), and toreva blocks according to the map (Ponomareva et al., 2006).

stratovolcanoes (Melekestsev et al., 1991b). The sequence of activity of Kamen and its neighbouring volcanoes is summarized in Fig. 3, based on geochronological evidence (Melekestsev et al., 1970, 1974; Melekestsev, 1980; Melekestsev and Braitseva, 1988; Braitseva et al., 1991; Flerov and Ovsyannikov, 1991; Braitseva et al., 1995; Calkins, 2004).

The chemical compositions of Kamen lavas show an evolution from earlier Ol-rich lavas, followed by Ol–Cpx–Pl-phyric lavas with

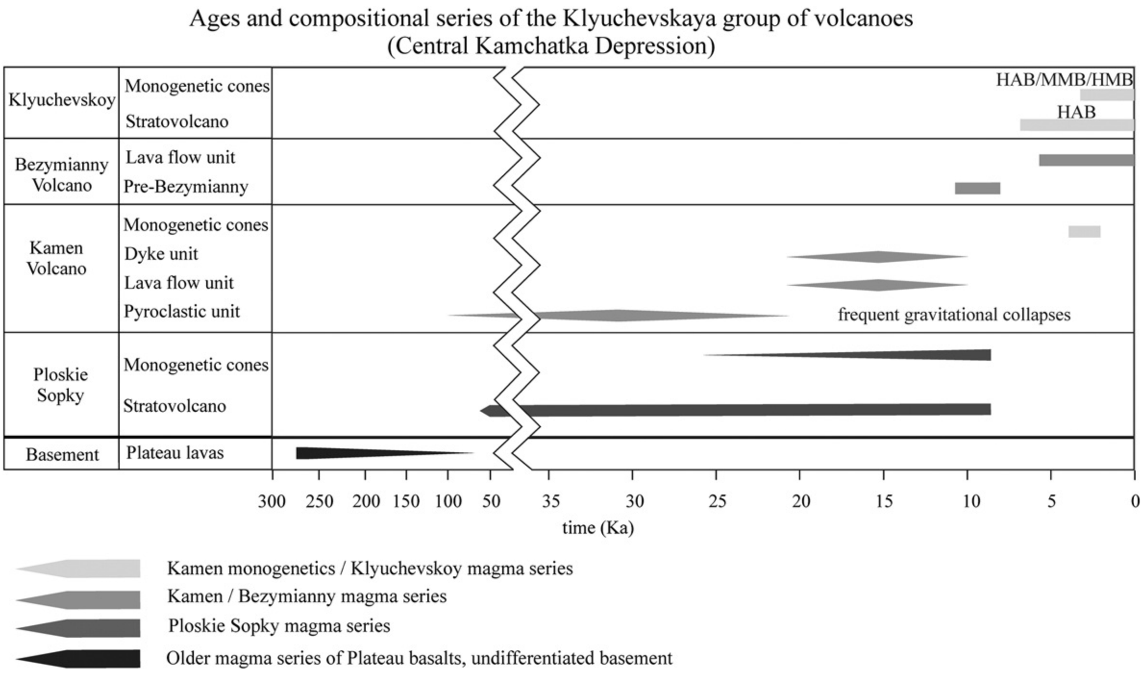


**Fig. 3.** Age-distribution diagram of Kamen Volcano and its surrounding stratovolcanoes and monogenetic centres. Age data are from (Melekestsev et al., 1970, 1974; Melekestsev, 1980; Melekestsev and Braitseva, 1988; Braitseva et al., 1991; Flerov and Ovsyannikov, 1991; Braitseva et al., 1995; Calkins, 2004). HAB — high-aluminium basalts; MMB — moderate-magnesium basalts; HMB — high-magnesium basalts.

**Table 1**
Major and trace element abundances in representative sets of Kamen rocks and plateau lavas.

| Sample | KAM-07-04 | KAM-07-14 | KAM-07-15 | KAM-07-16 | KAM-07-23 | KAM-07-24 | KAM-08-07 | KAM-08-39 | KAM-08-43 |
|---|---|---|---|---|---|---|---|---|---|
| Complex | Stratovolcano | Stratovolcano | Stratovolcano | Stratovolcano | Stratovolcano | Stratovolcano | Stratovolcano | Stratovolcano | Stratovolcano |
| Lat (N) | 55°58′52.7″ | 55°59′16.3″ | 55°59′35.3″ | 55°59′42.6″ | 55°59′3,4″ | 55°59′5,3″ | 56°0′2.9″ | 56°1′21.3″ | 56°1′15.2″ |
| Long (E) | 160°33′20.3″ | 160°32′36.9″ | 160°32′41.9″ | 160°32′49.6″ | 160°34′10,1″ | 160°34′4,7″ | 160°32′22.2″ | 160°31′48.8″ | 160°33′31.6″ |
| $SiO_2$ | 56.26 | 53.71 | 54.33 | 54.92 | 52.40 | 52.93 | 52.54 | 54.18 | 54.82 |
| $TiO_2$ | 0.91 | 1.02 | 0.95 | 1.01 | 1.07 | 1.13 | 1.05 | 0.93 | 0.88 |
| $Al_2O_3$ | 17.61 | 17.80 | 17.17 | 17.54 | 18.67 | 18.39 | 17.91 | 18.40 | 18.84 |
| FeO | 7.79 | 8.82 | 8.43 | 8.21 | 9.03 | 9.11 | 9.34 | 8.38 | 8.31 |
| MnO | 0.16 | 0.18 | 0.16 | 0.17 | 0.18 | 0.18 | 0.18 | 0.17 | 0.17 |
| MgO | 4.50 | 5.50 | 5.85 | 5.22 | 5.35 | 5.03 | 5.79 | 4.95 | 4.17 |
| CaO | 7.95 | 8.62 | 8.91 | 8.31 | 9.17 | 9.03 | 9.35 | 8.63 | 8.16 |
| $Na_2O$ | 3.43 | 3.21 | 3.16 | 3.34 | 3.26 | 3.24 | 2.93 | 3.31 | 3.51 |
| $K_2O$ | 1.18 | 0.94 | 0.88 | 1.09 | 0.70 | 0.76 | 0.75 | 0.88 | 0.95 |
| $P_2O_5$ | 0.21 | 0.19 | 0.17 | 0.19 | 0.18 | 0.20 | 0.16 | 0.17 | 0.18 |
| Sum | 100 | 100 | 100 | 100 | 100 | 100 | 100 | 100 | 100 |
| Li | 14.75 | 14.36 | 14.44 | 17.45 | 11.17 | 10.35 | 9.32 | 11.96 | 15.26 |
| Be | 0.67 | 0.61 | 0.59 | 0.7 | 0.55 | 0.6 | 0.54 | 0.51 | 0.62 |
| Sc | 25 | 29 | 34 | 29 | 30 | 31 | 34 | 27 | 23 |
| V | 216 | 254 | 272 | 239 | 263 | 283 | 298 | 235 | 207 |
| Cr | 21 | 15 | 99 | 38 | 31 | 24 | 56 | 37 | 16 |
| Co | 27 | 29 | 29 | 30 | 29 | 26 | 32 | 28 | 28 |
| Ni | 19 | 18 | 25 | 32 | 16 | 10 | 21 | 20 | 18 |
| Cu | 48 | 48 | 53 | 77 | 69 | 45 | 43 | 57 | 68 |
| Zn | 83 | 89 | 82 | 84 | 87 | 93 | 90 | 84 | 88 |
| Ga | 19 | 18 | 18 | 18 | 19 | 19 | 19 | 18 | 19 |
| Rb | 19.52 | 15.27 | 14.66 | 16.98 | 9.51 | 11.15 | 10.72 | 13.48 | 14.64 |
| Sr | 372 | 299 | 332 | 331 | 314 | 324 | 286 | 316 | 336 |
| Y | 20.07 | 22.61 | 19.4 | 20.28 | 22.68 | 24.06 | 22.34 | 21.87 | 22.25 |
| Zr | 101 | 97 | 87 | 91 | 86 | 91 | 80 | 89 | 97 |
| Nb | 2.07 | 1.87 | 1.79 | 1.94 | 1.95 | 2.03 | 1.68 | 1.71 | 1.79 |
| Mo | 1.01 | 0.8 | 0.87 | 0.67 | 0.63 | 0.93 | 0.94 | 0.55 | 0.66 |
| Cd | 0.12 | 0.11 | 0.11 | 0.12 | 0.11 | 0.14 | 0.1 | 0.12 | 0.11 |
| Sn | 0.9 | 0.87 | 0.71 | 0.82 | 0.83 | 0.89 | 0.79 | 0.8 | 0.86 |
| Sb | 0.21 | 0.16 | 0.13 | 0.2 | 0.09 | 0.1 | 0.11 | 0.16 | 0.13 |
| Cs | 0.41 | 0.39 | 0.34 | 0.43 | 0.31 | 0.37 | 0.26 | 0.38 | 0.44 |
| Ba | 451 | 325 | 304 | 419 | 207 | 244 | 284 | 285 | 312 |
| La | 9.58 | 7.26 | 7.46 | 7.75 | 6.39 | 6.72 | 5.72 | 7.24 | 7.59 |
| Ce | 19.31 | 15.79 | 15.33 | 16.35 | 14.41 | 15.02 | 12.78 | 15.18 | 15.98 |
| Pr | 2.89 | 2.5 | 2.36 | 2.55 | 2.33 | 2.43 | 2.07 | 2.32 | 2.43 |
| Nd | 14.13 | 12.81 | 11.66 | 12.82 | 12.07 | 12.69 | 10.75 | 11.74 | 12.15 |
| Sm | 3.62 | 3.56 | 3.17 | 3.48 | 3.49 | 3.6 | 3.12 | 3.13 | 3.25 |
| Eu | 1.14 | 1.17 | 1.05 | 1.13 | 1.21 | 1.23 | 1.08 | 1.09 | 1.12 |
| Gd | 4.01 | 4.13 | 3.67 | 3.95 | 4.1 | 4.3 | 3.88 | 3.8 | 3.89 |
| Tb | 0.6 | 0.66 | 0.58 | 0.63 | 0.67 | 0.71 | 0.64 | 0.62 | 0.63 |
| Dy | 3.97 | 4.49 | 3.88 | 4.14 | 4.52 | 4.66 | 4.32 | 4.09 | 4.16 |
| Ho | 0.79 | 0.9 | 0.77 | 0.82 | 0.91 | 0.96 | 0.89 | 0.85 | 0.87 |
| Er | 2.35 | 2.72 | 2.33 | 2.46 | 2.77 | 2.9 | 2.71 | 2.55 | 2.64 |
| Tm | 0.32 | 0.37 | 0.31 | 0.33 | 0.37 | 0.39 | 0.37 | 0.35 | 0.36 |
| Yb | 2.16 | 2.53 | 2.14 | 2.29 | 2.6 | 2.73 | 2.55 | 2.45 | 2.58 |
| Lu | 0.32 | 0.37 | 0.31 | 0.33 | 0.39 | 0.4 | 0.38 | 0.37 | 0.4 |
| Hf | 3 | 2.84 | 2.46 | 2.67 | 2.48 | 2.61 | 2.3 | 2.6 | 2.81 |
| Ta | 0.12 | 0.11 | 0.1 | 0.11 | 0.11 | 0.12 | 0.1 | 0.1 | 0.11 |
| W | 0.12 | 0.07 | 0.07 | 0.1 | 0.05 | 0.06 | 0.06 | 0.07 | 0.1 |
| Tl | 0.09 | 0.07 | 0.07 | 0.09 | 0.04 | 0.05 | 0.04 | 0.07 | 0.04 |
| Pb | 3.51 | 2.95 | 2.58 | 2.98 | 2.07 | 2.5 | 2.22 | 2.72 | 3.02 |
| Th | 0.79 | 0.58 | 0.69 | 0.57 | 0.35 | 0.51 | 0.46 | 0.62 | 0.63 |
| U | 0.54 | 0.39 | 0.52 | 0.43 | 0.3 | 0.46 | 0.41 | 0.44 | 0.44 |

All major elements and Sc, V, Cr, Co, Ni, Zn, Ga, Sr, Zr, Ba are determined by XRF (X-ray fluorescence spectrometry). Others values come from the ICP-MS (inductively coupled plasma mass spectrometry) analyses. Major elements are presented in wt.%, trace elements — in ppm.

[a] Cone — lava flow from the monogenetic cone.

[b] KGV — Klyuchevskaya group of volcanoes. Sample PLAT-08-01 was collected in Klyuchi settlement.

[c] Sample PLAT-08-02 was collected in Kozyrevsk settlement.

[d] Sample BEZ-09-04 was collected near Plotina camp.

decreasing amounts of mafic minerals. The upper parts of the stratovolcano are characterised by Ol-free lavas and rare Hbl-bearing andesite lavas. However, there are some exceptions to this general trend; for example, there is an outcrop of Hbl andesite lavas at the base of the collapse wall at an altitude of 1680 m.

The numerous dikes that crosscut the older edifice form a radial pattern as well as ring structures in all sectors of the edifice. Their thickness ranges from 1 to 5 m and they reach up to 2 km in length. Most dikes are petrographically similar to the younger stratovolcano lavas. However, Ol-rich dikes with 20–25% of large Ol phenocrysts

| KAM-08-97 | KAM 09-07 | KAM-09-11 | KAM-09-15 | KAM 09-36 | KAM 09-39 | KAM 09-55 | KAM-09-65 | KAM-07-19 |
|---|---|---|---|---|---|---|---|---|
| Stratovolcano | Stratovolcano | Stratovolcano | Stratovolcano | Stratovolcano | Stratovolcano | Stratovolcano | Stratovolcano | Dike |
| 55°57′49.7″ | 55°59′9.9″ | 55°59′12.9″ | 56°0′46.1″ | N 55°58′59.5″ | 55°59′19.7″ | 55°56′21.5″ | 55°57′10″ | 55°59′39.1″ |
| 160°40′57.8″ | 160°37′41.3″ | 160°37′46.6″ | 160°38′27.4″ | 160°39′52.3″ | 160°38′22.3″ | 160°39′24.8″ | 160°37′5.3″ | 160°32′17.6″ |
| 55.26 | 55.91 | 55.15 | 53.43 | 53.36 | 57.97 | 52.36 | 52.99 | 52.25 |
| 0.88 | 0.88 | 0.96 | 0.98 | 0.98 | 0.80 | 1.09 | 1.11 | 1.09 |
| 18.69 | 17.66 | 17.96 | 16.43 | 15.56 | 17.73 | 17.80 | 18.24 | 17.99 |
| 8.00 | 7.72 | 7.92 | 8.72 | 8.47 | 6.50 | 9.17 | 8.81 | 9.15 |
| 0.16 | 0.16 | 0.16 | 0.18 | 0.17 | 0.14 | 0.18 | 0.17 | 0.18 |
| 4.16 | 4.89 | 4.82 | 6.83 | 7.93 | 4.19 | 6.03 | 5.37 | 5.90 |
| 8.11 | 7.97 | 8.31 | 9.36 | 9.40 | 7.23 | 9.32 | 9.02 | 9.40 |
| 3.54 | 3.57 | 3.42 | 2.98 | 3.02 | 3.92 | 3.21 | 3.35 | 3.18 |
| 0.99 | 1.03 | 1.10 | 0.90 | 0.92 | 1.30 | 0.67 | 0.74 | 0.68 |
| 0.21 | 0.20 | 0.20 | 0.19 | 0.19 | 0.21 | 0.19 | 0.19 | 0.18 |
| 100 | 100 | 100 | 100 | 100 | 100 | 100 | 100 | 100 |
| 17.07 | 16.23 | 14.39 | 10.27 | 11.7 | 19.39 | 10.83 | 13.01 | 11.01 |
| 0.66 | 0.65 | 0.62 | 0.51 | 0.6 | 0.78 | 0.54 | 0.53 | 0.56 |
| 20 | 26 | 26 | 34 | 34 | 22 | 32 | 29 | 31 |
| 189 | 199 | 226 | 261 | 246 | 183 | 263 | 271 | 271 |
| 12 | 71 | 48 | 152 | 319 | 58 | 71 | 47 | 73 |
| 24 | 27 | 27 | 34 | 36 | 23 | 32 | 29 | 31 |
| 15 | 42 | 28 | 44 | 72 | 40 | 24 | 19 | 22 |
| 51 | 65 | 62 | 67 | 64 | 66 | 51 | 50 | 55 |
| 89 | 86 | 83 | 84 | 79 | 79 | 87 | 88 | 87 |
| 19 | 19 | 18 | 18 | 17 | 18 | 18 | 19 | 18 |
| 15.43 | 16.17 | 19.01 | 14.8 | 15.72 | 22.62 | 9.29 | 10.32 | 9.8 |
| 327 | 412 | 329 | 345 | 317 | 398 | 313 | 318 | 321 |
| 21.57 | 20.07 | 20.38 | 18.98 | 19.32 | 17.74 | 21.13 | 21.45 | 23.06 |
| 100 | 98 | 96 | 88 | 93 | 110 | 92 | 94 | 88 |
| 2.02 | 2.06 | 2.24 | 1.81 | 2.11 | 2.44 | 2.1 | 2.24 | 1.94 |
| 0.75 | 0.62 | 0.65 | 0.82 | 0.7 | 0.8 | 0.76 | 0.71 | 0.79 |
| 0.11 | 0.11 | 0.1 | 0.08 | 0.09 | 0.09 | 0.11 | 0.1 | 0.13 |
| 0.85 | 0.77 | 0.83 | 0.79 | 0.81 | 0.76 | 0.82 | 0.97 | 0.81 |
| 0.13 | 0.16 | 0.18 | 0.1 | 0.11 | 0.27 | 0.07 | 0.11 | 0.1 |
| 0.45 | 0.27 | 0.54 | 0.34 | 0.42 | 0.65 | 0.27 | 0.22 | 0.31 |
| 367 | 425 | 398 | 348 | 317 | 481 | 199 | 237 | 211 |
| 8.83 | 9.95 | 8.45 | 8.64 | 8.27 | 10.5 | 6.6 | 6.87 | 6.63 |
| 18.03 | 20 | 17.55 | 18.07 | 17.38 | 20.82 | 14.81 | 15.33 | 14.89 |
| 2.76 | 3.02 | 2.71 | 2.76 | 2.65 | 3.08 | 2.37 | 2.44 | 2.39 |
| 13.52 | 14.71 | 13.37 | 13.57 | 13.16 | 14.65 | 12.24 | 12.57 | 12.5 |
| 3.52 | 3.69 | 3.56 | 3.57 | 3.52 | 3.56 | 3.5 | 3.63 | 3.54 |
| 1.2 | 1.23 | 1.2 | 1.18 | 1.16 | 1.16 | 1.21 | 1.22 | 1.21 |
| 4.09 | 4.08 | 4.04 | 3.98 | 3.97 | 3.8 | 4.11 | 4.21 | 4.2 |
| 0.65 | 0.63 | 0.65 | 0.63 | 0.63 | 0.59 | 0.69 | 0.7 | 0.68 |
| 4.21 | 4.07 | 4.2 | 4.03 | 4.07 | 3.69 | 4.5 | 4.58 | 4.55 |
| 0.86 | 0.82 | 0.85 | 0.81 | 0.82 | 0.74 | 0.91 | 0.93 | 0.93 |
| 2.61 | 2.47 | 2.56 | 2.44 | 2.49 | 2.25 | 2.78 | 2.84 | 2.8 |
| 0.36 | 0.33 | 0.35 | 0.32 | 0.33 | 0.3 | 0.37 | 0.38 | 0.37 |
| 2.5 | 2.31 | 2.38 | 2.23 | 2.26 | 2.1 | 2.55 | 2.6 | 2.61 |
| 0.38 | 0.34 | 0.35 | 0.32 | 0.33 | 0.31 | 0.37 | 0.38 | 0.38 |
| 2.91 | 2.99 | 2.87 | 2.6 | 2.68 | 3.22 | 2.6 | 2.77 | 2.54 |
| 0.11 | 0.12 | 0.13 | 0.1 | 0.11 | 0.14 | 0.11 | 0.12 | 0.13 |
| 0.09 | 0.1 | 0.09 | 0.09 | 0.08 | 0.31 | 0.06 | 0.08 | 0.05 |
| 0.07 | 0.06 | 0.06 | 0.04 | 0.08 | 0.08 | 0.03 | 0.04 | 0.05 |
| 2.94 | 3 | 2.82 | 2.35 | 2.45 | 3.65 | 1.84 | 1.87 | 2.11 |
| 0.68 | 0.79 | 0.66 | 0.62 | 0.61 | 0.89 | 0.36 | 0.41 | 0.4 |
| 0.46 | 0.45 | 0.44 | 0.38 | 0.36 | 0.59 | 0.3 | 0.34 | 0.34 |

(continued on next page)

(>3 mm) and abundant Hbl-rich andesites were also found on the E and SW slopes of the volcano.

Presumably Kamen Volcano terminated its activity 10 to 11 ka ago because no younger Kamen rocks are present (Melekestsev and Braitseva, 1988). Since then, the edifice has been destroyed by numerous gravitational collapses (Ponomareva et al., 2006), leaving large toreva blocks – intact fragments of the collapsed volcanic edifice (Reiche, 1937) – as well as widespread debris avalanche deposits. About 11 ka ago (Braitseva et al., 1991) Bezymianny Volcano started to form on the southern slope of the now-extinct Kamen Volcano.

**Table 1** (*continued*)

| Sample | KAM-08-30 | KAM-08-50 | KAM-08-84 | KAM-08-A1 | KAM 09-04 | KAM 09-08 | KAM 09-09 | KAM 09-45 |
|---|---|---|---|---|---|---|---|---|
| Complex | Dike | Dike | Dike | Dike | Dike | Dike | Dike | Dike |
| Lat (N) | 55°59′50″ | 56°0′56.5″ | 55°57′39.8″ | 55°58′54.2″ | 55°59′34.4″ | 55°59′14.8″ | 55°59′14.8″ | 55°59′21.3″ |
| Long (E) | 160°32′9.6″ | 160°31′57.1″ | 160°42′57.4″ | 160°41′12.6″ | 160°39′2.2″ | 160°37′37.4″ | 160°37′37.4″ | 160°38′13.7″ |
| $SiO_2$ | 61.25 | 53.46 | 53.20 | 53.08 | 54.13 | 54.79 | 53.90 | 53.39 |
| $TiO_2$ | 0.59 | 1.07 | 1.03 | 1.11 | 0.95 | 1.03 | 1.02 | 0.94 |
| $Al_2O_3$ | 17.46 | 18.37 | 17.82 | 18.54 | 16.42 | 17.78 | 17.20 | 16.16 |
| FeO | 5.41 | 8.92 | 8.78 | 8.86 | 8.37 | 8.33 | 8.46 | 8.75 |
| MnO | 0.12 | 0.18 | 0.18 | 0.17 | 0.17 | 0.16 | 0.17 | 0.18 |
| MgO | 3.21 | 4.97 | 5.66 | 5.11 | 6.50 | 5.07 | 5.88 | 7.36 |
| CaO | 6.45 | 8.77 | 9.13 | 8.79 | 9.07 | 8.27 | 8.81 | 9.35 |
| $Na_2O$ | 4.06 | 3.20 | 3.28 | 3.41 | 3.16 | 3.34 | 3.28 | 2.93 |
| $K_2O$ | 1.27 | 0.89 | 0.73 | 0.74 | 1.04 | 1.03 | 1.09 | 0.77 |
| $P_2O_5$ | 0.18 | 0.19 | 0.19 | 0.19 | 0.18 | 0.19 | 0.18 | 0.17 |
| Sum | 100 | 100 | 100 | 100 | 100 | 100 | 100 | 100 |
| Li | 14 | 11.6 | 10.44 | 12.14 | 15.69 | 14.48 | 15.35 | 14.26 |
| Be | 0.77 | 0.42 | 0.52 | 0.48 | 0.61 | 0.62 | 0.64 | 0.58 |
| Sc | 18 | 28 | 30 | 27 | 31 | 27 | 34 | 34 |
| V | 126 | 261 | 237 | 265 | 235 | 256 | 247 | 261 |
| Cr | 39 | 19 | 69 | 33 | 149 | 66 | 97 | 186 |
| Co | 17 | 30 | 29 | 28 | 32 | 28 | 33 | 36 |
| Ni | 23 | 17 | 24 | 17 | 44 | 18 | 39 | 57 |
| Cu | 33 | 56 | 50 | 46 | 81 | 36 | 88 | 64 |
| Zn | 70 | 91 | 88 | 89 | 84 | 85 | 87 | 84 |
| Ga | 17 | 19 | 18 | 20 | 17 | 19 | 18 | 18 |
| Rb | 22.84 | 12.23 | 10.95 | 9.99 | 15.1 | 17.46 | 16.06 | 16.11 |
| Sr | 406 | 310 | 322 | 324 | 303 | 333 | 315 | 309 |
| Y | 15.02 | 23.43 | 23.09 | 22.75 | 21.92 | 20.39 | 22.75 | 21.8 |
| Zr | 119 | 91 | 98 | 95 | 107 | 96 | 112 | 81 |
| Nb | 2.26 | 1.95 | 2.19 | 2.2 | 2.2 | 2.12 | 2.3 | 2.18 |
| Mo | 0.83 | 0.89 | 1.02 | 0.67 | 0.88 | 0.96 | 0.79 | 0.83 |
| Cd | 0.08 | 0.14 | 0.12 | 0.12 | 0.14 | 0.11 | 0.26 | 0.12 |
| Sn | 0.54 | 0.85 | 0.9 | 0.81 | 1.08 | 0.83 | 1.02 | 0.92 |
| Sb | 0.24 | 0.12 | 0.1 | 0.11 | 0.14 | 0.14 | 0.15 | 0.15 |
| Cs | 0.37 | 0.29 | 0.34 | 0.26 | 0.39 | 0.54 | 0.42 | 0.43 |
| Ba | 503 | 366 | 217 | 237 | 319 | 339 | 363 | 326 |
| La | 10.67 | 7.13 | 7.02 | 6.95 | 8 | 7.99 | 8.32 | 8.01 |
| Ce | 20.35 | 15.36 | 15.52 | 15.4 | 16.9 | 16.57 | 17.56 | 16.81 |
| Pr | 2.78 | 2.44 | 2.45 | 2.43 | 2.62 | 2.53 | 2.75 | 2.63 |
| Nd | 12.4 | 12.57 | 12.37 | 12.54 | 13.04 | 12.68 | 13.71 | 13.29 |
| Sm | 2.78 | 3.49 | 3.47 | 3.54 | 3.52 | 3.44 | 3.75 | 3.68 |
| Eu | 0.88 | 1.19 | 1.2 | 1.23 | 1.16 | 1.16 | 1.22 | 1.22 |
| Gd | 2.9 | 4.21 | 4.17 | 4.23 | 4.06 | 3.98 | 4.35 | 4.28 |
| Tb | 0.43 | 0.68 | 0.67 | 0.69 | 0.66 | 0.64 | 0.71 | 0.7 |
| Dy | 2.78 | 4.46 | 4.41 | 4.53 | 4.32 | 4.17 | 4.66 | 4.59 |
| Ho | 0.56 | 0.91 | 0.9 | 0.93 | 0.89 | 0.84 | 0.94 | 0.94 |
| Er | 1.71 | 2.76 | 2.73 | 2.8 | 2.66 | 2.56 | 2.85 | 2.85 |
| Tm | 0.23 | 0.37 | 0.37 | 0.38 | 0.36 | 0.34 | 0.38 | 0.38 |
| Yb | 1.69 | 2.62 | 2.59 | 2.61 | 2.5 | 2.35 | 2.65 | 2.64 |
| Lu | 0.26 | 0.39 | 0.39 | 0.39 | 0.37 | 0.35 | 0.39 | 0.39 |
| Hf | 3.22 | 2.63 | 2.73 | 2.72 | 3.06 | 2.78 | 3.19 | 2.83 |
| Ta | 0.14 | 0.11 | 0.12 | 0.12 | 0.12 | 0.12 | 0.13 | 0.12 |
| W | 0.11 | 0.06 | 0.07 | 2.57 | 0.07 | 0.09 | 0.06 | 0.09 |
| Tl | 0.05 | 0.05 | 0.05 | 0.04 | 0.07 | 0.09 | 0.08 | 0.06 |
| Pb | 3.85 | 2.86 | 2.31 | 2.06 | 2.63 | 2.62 | 2.44 | 3.04 |
| Th | 1.14 | 0.55 | 0.42 | 0.4 | 0.48 | 0.62 | 0.52 | 0.66 |
| U | 0.73 | 0.45 | 0.35 | 0.32 | 0.46 | 0.47 | 0.45 | 0.44 |

However, the eruption activity of this older part of Bezymianny Volcano (called Pre-Bezymianny (Braitseva et al., 1991)) did not peak until about 5.5 ka (Fig. 3). At around the same time, 7 ka ago (Braitseva et al., 1995), Klyuchevskoy Volcano started to form on the northern slope of Kamen Volcano. After about 2–3.5 ka BP (oral communication by O.A. Braitseva and V.V. Ponomareva) a series of monogenetic cones erupted along the western sector of Kamen Volcano. These cones are composed mainly of cinder but often produced lava flows as long as 5 km. The petrography of these rocks is rather mafic, with an Ol–Cpx–Pl phenocyrst assemblage.

| KAM-07-03 | KAM-07-11 | KAM-07-13 | KAM-08-01 | KAM-08-14 | KAM-08-20 | KAM-08-68 | PLAT-08-01 | PLAT-08-02 | BEZ-09-04 |
|---|---|---|---|---|---|---|---|---|---|
| Cone[a] | Cone | Cone | Cone | Cone | Cone | Cone | KGV plateau[b] | KGV plateau[c] | KGV plateau[d] |
| 55°58′4.2″ | 55°59.899″ | 55°58′17.5″ | 56°0′1.9″ | 55°59′59.7″ | 56°0′7″ | 55°59′50.5″ | 56°19′36.3″ | 56°3′25.3″ | 55°56′0.3″ |
| 160°31′32.1″ | 160°30.275″ | 160°28′59.7″ | 160°30′46″ | 160°29′19.3″ | 160°20′15.8″ | 160°29′58.5″ | 160°50′32.3″ | 159°52′0.6″ | 160°35′14″ |
| 52.82 | 53.02 | 52.46 | 52.96 | 53.93 | 52.25 | 52.99 | 55.01 | 53.65 | 52.66 |
| 0.91 | 0.89 | 0.96 | 0.90 | 1.04 | 1.11 | 0.91 | 1.48 | 1.34 | 1.65 |
| 17.39 | 15.07 | 17.32 | 15.11 | 17.94 | 16.70 | 15.16 | 17.85 | 18.22 | 17.92 |
| 8.46 | 8.61 | 8.73 | 8.67 | 8.29 | 8.86 | 8.68 | 8.26 | 8.62 | 8.58 |
| 0.16 | 0.17 | 0.17 | 0.17 | 0.16 | 0.17 | 0.17 | 0.15 | 0.15 | 0.16 |
| 6.89 | 8.81 | 6.65 | 8.78 | 5.39 | 7.04 | 8.70 | 3.53 | 3.82 | 3.77 |
| 9.25 | 9.76 | 9.67 | 9.69 | 8.44 | 9.76 | 9.66 | 7.74 | 8.52 | 8.20 |
| 3.25 | 2.79 | 3.20 | 2.81 | 3.69 | 3.19 | 2.81 | 3.50 | 3.65 | 3.72 |
| 0.70 | 0.73 | 0.67 | 0.75 | 0.93 | 0.74 | 0.76 | 1.94 | 1.64 | 2.56 |
| 0.16 | 0.16 | 0.16 | 0.16 | 0.19 | 0.19 | 0.16 | 0.53 | 0.38 | 0.79 |
| 100 | 100 | 100 | 100 | 100 | 100 | 100 | 100 | 100 | 100 |
| 10.05 | 10.84 | 11.2 | 9.91 | 12.91 | 8.41 | 10.14 | 22.9 | 19.91 | 19.35 |
| 0.48 | 0.53 | 0.49 | 0.45 | 0.59 | 0.56 | 0.43 | 1.48 | 1.17 | 2.17 |
| 30 | 34 | 34 | 37 | 29 | 34 | 35 | 22 | 22 | 23 |
| 238 | 248 | 264 | 250 | 245 | 268 | 252 | 287 | 302 | 259 |
| 162 | 428 | 92 | 414 | 58 | 124 | 400 | 20 | 41 | 62 |
| 34 | 38 | 34 | 39 | 31 | 35 | 39 | 25 | 26 | 24 |
| 65 | 101 | 48 | 106 | 37 | 51 | 107 | 30 | 25 | 27 |
| 76 | 102 | 109 | 64 | 92 | 97 | 89 | 193 | 157 | 256 |
| 79 | 77 | 81 | 79 | 86 | 81 | 79 | 90 | 90 | 95 |
| 18 | 16 | 19 | 16 | 19 | 17 | 17 | 20 | 19 | 20 |
| 10.81 | 12.54 | 10.58 | 12.78 | 15.17 | 11.38 | 12.84 | 49.28 | 32.83 | 73 |
| 340 | 275 | 345 | 277 | 341 | 309 | 278 | 414 | 433 | 380 |
| 18.44 | 17.85 | 19.01 | 17.96 | 20.53 | 21.31 | 18.18 | 29.54 | 24.4 | 31.44 |
| 82 | 80 | 81 | 82 | 98 | 97 | 82 | 220 | 155 | 237 |
| 1.58 | 1.55 | 1.55 | 1.59 | 1.9 | 2.12 | 1.61 | 5.23 | 3.54 | 8.01 |
| 0.7 | 0.74 | 0.58 | 0.72 | 0.73 | 0.73 | 0.77 | 2.34 | 1.83 | 2.18 |
| 0.09 | 0.09 | 0.1 | 0.09 | 0.07 | 0.09 | 0.09 | 0.08 | 0.06 | 0.04 |
| 0.69 | 0.68 | 0.66 | 0.7 | 0.9 | 0.88 | 0.73 | 1.73 | 1.37 | 2.19 |
| 0.13 | 0.17 | 0.1 | 0.18 | 0.18 | 0.13 | 0.18 | 0.48 | 0.28 | 0.35 |
| 0.21 | 0.43 | 0.35 | 0.46 | 0.49 | 0.37 | 0.43 | 1.54 | 0.96 | 2.06 |
| 242 | 266 | 243 | 279 | 389 | 235 | 269 | 638 | 520 | 560 |
| 6.48 | 6.3 | 6.34 | 6.29 | 8.11 | 7.17 | 6.25 | 21.67 | 15.67 | 27.43 |
| 13.78 | 13.52 | 13.73 | 13.6 | 16.92 | 15.7 | 13.41 | 43.28 | 32.17 | 54.83 |
| 2.13 | 2.07 | 2.15 | 2.1 | 2.61 | 2.41 | 2.05 | 6.34 | 4.76 | 7.82 |
| 10.69 | 10.45 | 10.85 | 10.43 | 12.97 | 12.3 | 10.35 | 29.74 | 23.22 | 36.06 |
| 2.93 | 2.88 | 3.07 | 2.91 | 3.43 | 3.32 | 2.8 | 7.03 | 5.59 | 7.95 |
| 1.01 | 0.96 | 1.05 | 0.96 | 1.14 | 1.13 | 0.96 | 1.81 | 1.64 | 2.09 |
| 3.45 | 3.38 | 3.55 | 3.34 | 3.9 | 3.96 | 3.43 | 7 | 5.7 | 7.61 |
| 0.52 | 0.53 | 0.56 | 0.54 | 0.62 | 0.63 | 0.54 | 1.05 | 0.87 | 1.13 |
| 3.56 | 3.55 | 3.78 | 3.51 | 4.01 | 4.09 | 3.49 | 6.53 | 5.41 | 6.92 |
| 0.7 | 0.7 | 0.75 | 0.71 | 0.81 | 0.83 | 0.7 | 1.27 | 1.07 | 1.37 |
| 2.11 | 2.08 | 2.23 | 2.11 | 2.41 | 2.46 | 2.1 | 3.84 | 3.21 | 4.18 |
| 0.28 | 0.28 | 0.3 | 0.28 | 0.32 | 0.33 | 0.28 | 0.5 | 0.41 | 0.55 |
| 1.91 | 1.89 | 2.04 | 1.98 | 2.23 | 2.29 | 1.95 | 3.46 | 2.89 | 3.82 |
| 0.28 | 0.28 | 0.3 | 0.29 | 0.33 | 0.34 | 0.29 | 0.49 | 0.42 | 0.55 |
| 2.34 | 2.37 | 2.29 | 2.36 | 2.82 | 2.7 | 2.34 | 6.28 | 4.64 | 6.56 |
| 0.09 | 0.09 | 0.09 | 0.09 | 0.11 | 0.12 | 0.09 | 0.29 | 0.19 | 0.42 |
| 0.07 | 0.09 | 0.05 | 0.09 | 0.09 | 0.08 | 0.09 | 0.28 | 0.56 | 0.38 |
| 0.04 | 0.05 | 0.05 | 0.05 | 0.06 | 0.04 | 0.04 | 0.09 | 0.05 | 0.05 |
| 2.67 | 2.85 | 2.34 | 2.83 | 3.36 | 2.57 | 2.69 | 7.12 | 5.26 | 6.48 |
| 0.55 | 0.55 | 0.49 | 0.57 | 0.76 | 0.55 | 0.5 | 2.44 | 1.58 | 2.97 |
| 0.36 | 0.38 | 0.31 | 0.41 | 0.47 | 0.37 | 0.37 | 1.43 | 0.97 | 1.68 |

The last known event from Kamen Volcano happened 1200 years ago (Melekestsev and Braitseva, 1988; Ponomareva et al., 2006) when the eastern slope of the volcano was destroyed by the largest Holocene gravitational collapse in Kamchatka; this collapse, with a volume of 6 km$^3$ (Figs. e-1, 2), created the so-called "Ambon" deposits. The remaining N–NW sector of Kamen Volcano is completely covered by glaciers. The collapse 1200 years ago cut the edifice of the volcano and exposed its inner part as a vertical wall 2.5 km high. Our study indicates that about 80% of the wall is composed of well-stratified pyroclastic deposits cut by numerous dikes. Thin lava flows are rare in this section;

they are located mainly in the upper part of the edifice and occurred during the final stage of stratovolcano formation. These deposits are represented by moderately indurated volcanic breccias. Representative outcrops of such deposits can be found mainly at the base of the collapse wall and in North Griva toreva block and two unnamed toreva blocks at the eastern part of the volcano. The breccias mainly consist of poorly-sorted coarse-grained deposits of mostly angular, dense blocks, 2 m and more in diameter. The great thicknesses of the pyroclastic deposits, up to 600 m (approx. 80% of the stratocone volume), testify that a significant part of Kamen Volcano history is characterised by explosive activity.

The colour of the collapse wall pyroclastic deposits ranges from fresh black-grey deposits at the flanks of the edifice to yellow, grey-green, and finally red towards the centre (e-Fig. 1). Such variations in colour are likely the result of increased thermal and/or hydrothermal flux in the central parts of the volcano.

The Ambon collapse deposits are composed of the same varied lithologies and colours as observed in the collapse scar: volcanic breccia and tuffs with blocks and a matrix composed of lapilli and altered argillaceous ash. In addition, some Ambon deposit blocks are composed of pyroclastic material and compounded fragments of large (>50 m) lava blocks that make these blocks more resistant to erosion. Two toreva blocks situated in the lower part of the Shmidt glacier at the axis of the collapse did not break up during the collapse and subsequent erosion because they were protected by long (2.5 km) dikes of Ol–Cpx basaltic andesites, and because they were covered by lava flows. Other blocks in the debris avalanche are completely destroyed and reduced to small conical hills only a few metres tall composed only of fine-grained hydrothermally-altered pyroclastic lapilli-tuffs. Such extensive hydrothermal alteration in the debris blocks clearly pre-dates the collapse event; thus, weakening of the edifice by internal hydrothermal alteration may have been the principal cause of collapse.

Three stratigraphic suites define the volcanic history of Kamen:

(1) The oldest, mostly pyroclastic sequence that built most of the collapsed edifice;
(2) Younger lavas and dikes that form the upper sections of the stratovolcano or crosscut the older pyroclastic deposits;
(3) Monogenetic cones and associated lava flows.

We will discuss the petrographic, mineralogical, and geochemical characteristics of these main suites below.

## 3. Analytical techniques

Major and trace elements of whole rocks were analysed at Geoscience Centre (GZG), Göttingen University and are presented in Table 1 and e-Table 1. Major and some trace elements (Sc, V, Cr, Co, Ni, Zn, Ga, Sr, Zr, Ba) in 88 samples were determined by standard X-ray fluorescence (XRF) analysis on glass discs prepared with a sodium tetraborate flux. Analytical errors for major elements are around 1% (except for Fe, Na: 2% and LOI: ~10%) and for trace elements around 5%.

In addition, 38 samples were analysed by inductively coupled plasma mass spectrometry (ICPMS). About 100 mg samples of whole rock powder were dissolved in teflon beakers with a mixture of HF and $HClO_4$ under pressure, and after evaporation were redissolved in $HNO_3$ for the measurement. The international JA2 standard was analysed continuously together with samples to check the external reproducibility. From this we estimate the error for Nb and Ta to be about 15–20%; for all other trace elements the error is lower than 10%.

The composition of the rock-forming minerals in basalts from Kamen and neighbouring Klyuchevskoy and Ploskie Sopky volcanoes was determined using routine procedures for microprobe analyses on a JEOL JXA 8900RL instrument at the GZG. This instrument was equipped with 5 wavelength dispersive spectrometer (WDS) detectors, run at 15 kV and 15 nA with a 5–10 μm beam diameter. Peak counting times for major elements were 15–30 s, and for trace elements 60 s. For standardization, we used a set of synthetic and natural standards. Analytical precision was better than 5% for most major elements and 7% for K and P. The detailed description of the analytical procedure can be found in Ginibre et al. (2002) and Churikova et al. (2007).

The chemical composition of the minerals and matrix glasses in rocks from monogenetic cones and dikes was determined at Lomonosov

**Table 2**
Petrographic features of Kamen Volcano rocks.

| Rock group | Rock type | Structures | Location | Ol | Cpx | Opx | Pl | Hb | Mt/Ti–Mt | Sum of mafic minerals | Comments |
|---|---|---|---|---|---|---|---|---|---|---|---|
| Ol-bearing | Ol-Cpx | Porphyric and series-porphyric | Stratovolcano, dikes, monogenetic cones | + | + | − | +/− | − | + | 5–20% | Ol/Cpx ratio shows significant variation. The grains of Ol and Cpx are usually idiomorphic and often zoned. Pl phenocrysts are often resorbed. In monogenetic cones large Ol phenocrysts dominates over Cpx, in stratovolcano lavas and dikes Cpx is larger and dominates over Ol. Groundmass varies from light grey to almost black depending on crystallinity and alteration. |
| | Ol-2Px | Porphyric with middle and large phenocrysts | Low part of stratovolcano, dikes | + | + | + | − | − | + | 10–25% | Ol/Cpx ratio changes from olivine-rich rocks to essentially pyroxene-rich lavas. Cpx and Opx form glomeroporphyres with crystals 10–15 mm in size. Some Cpx grains are zoned and resorbed. |
| Ol-free | 2PX-Pl | Porphyric with middle and large phenocrysts | NW part of stratovolcano | − | + | + | + | − | + | <30% | Pl dominates, Opx can be large in size and comprises up to 30% of the rock. |
| | Cpx-Pl | Porphyric | Stratovolcano | +/− | + | − | + | − | + | 5–8% | Cpx form large (up to 8–10 mm), often zoned grains. Pl form elongated prisms, 2–3 mm in size, often zoned and resorbed. Pl usually dominate over Cpx. |
| | Pl | Series-porphyric | Stratovolcano | +/− | +/− | − | + | − | + | <1% | Mafic minerals are less than 1–3 mm. |
| Subaphyric rocks | | Aphyric structure | Stratovolcano, monogenetic cones | − | − | − | − | − | − | | |
| Hb-bearing | | Porphyric | Upper part of stratovolcano, basement of eastern collapse wall, dikes in SW sector | +/− | +/− | +/− | + | + | + | From single grains to 5–7% | Hb-bearing rocks are very rare. Hb has thick opacite-magnetite rim. Often Hb is replaced by secondary minerals. |

Moscow State University by electron microscope (Jeol JSM-6480LV equipped with an energy-dispersive INCA-Energy 350 spectrometer). The samples were analysed after 30 nm carbon sputtering at 15 kV and 15 nA. The processing of the results was conducted using professional SEM Control User Interface software, version 7.11 (Jeol Technics LTD) and INCA, version 17a (Oxford Instrument). Sample current calibration was carried out using a cobalt target. Analysis precision for most major elements at concentrations of 1–5 wt.% is less than 10% relative, at concentrations of 5–10 wt.% less than 5% relative, and at concentrations > 10 wt.% the error is less than 2% relative.

## 4. Results and discussion

### 4.1. Petrography

Kamen Volcano rocks are lavas and clastic rocks with various vesicularities and phenocryst abundances (Table 2). The rock structures change from subaphyric and series-porphyric to Ol and Cpx mega-porphyric. Interestingly, mega-plagiophyric rocks, like those at the plateau lavas below the KGV and at some KGV, were not found at Kamen Volcano. The main phenocrysts in stratovolcano rocks are Ol, Cpx, Opx, Pl, ilmenite, magnetite, and rare Hbl.

Based on petrographical and mineralogical features, Kamen Volcano rocks can be divided into four groups (Table 2). There are Ol-bearing rocks (Ol–2Px and Ol–Cpx), Ol-free lavas (2Px–Pl, Cpx–Pl, and Pl), and subaphyric and Hbl-bearing samples (Table 2). All these types occur throughout the stratigraphy of Kamen Volcano. However, monogenetic cones consist primarily of Ol-bearing and subaphyric rocks. Samples from the dike complex are Ol- and Hbl-bearing.

### 4.2. Mineral compositions

An electron microprobe was used to analyse 200 phenocryst grains of Ol, 145 of Cpx, and 49 of Pl from two representative samples of Kamen stratovolcano and one Ol–Cpx dike as well as two lavas from monogenetic cones (Fig. 4). Representative analyses are given in Table 3 and the full set of analyses is presented in e-Table 2. In addition to our new data, we also include previously published data (Almeev, 2005; Ivanov, 2008) in our discussion.

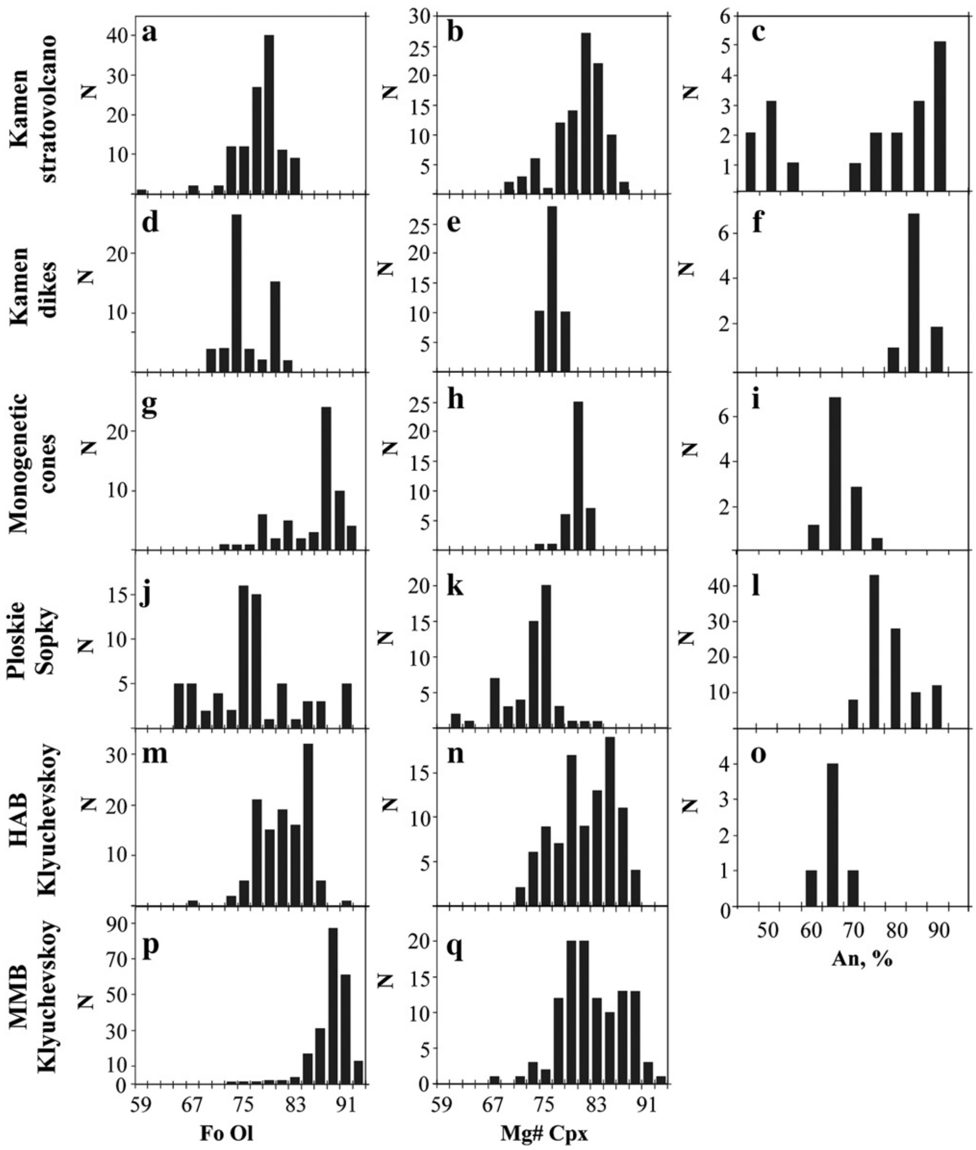


**Fig. 4.** Range of mineral composition in samples from Kamen Volcano and neighbouring volcanoes. Kamen Volcano: (*a–c*) — stratovolcano, (*d–f*) — dikes, (*g–i*) — monogenetic cones; Ploskie Sopky Volcano (*j–l*); Klyuchevskoy Volcano: (*m–o*) — high-Al basalts (HAB), (*p–q*) — moderate-Mg basalts (MMB). Histograms show the Ol, Cpx, and Pl compositions based on their forsterite (Fo), Mg/(Mg + Fe) (Mg#), and anorthite (An) component.

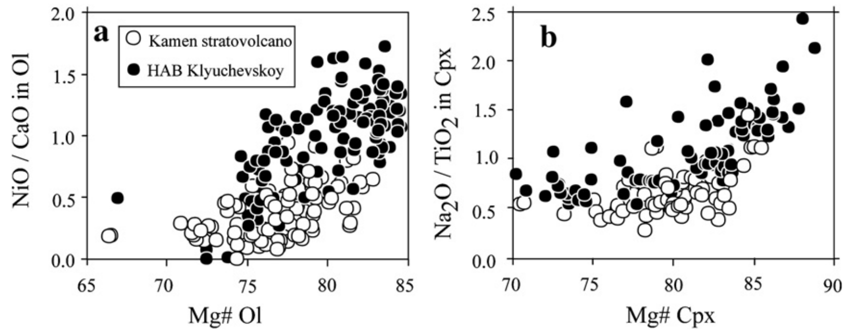


**Fig. 5.** Trace element ratios in Ol and Cpx from Kamen Volcano and from high-Al basalts (HAB) of Klyuchevskoy Volcano: a — NiO/CaO ratio in Ol vs. Ol Mg#; b — $Na_2O/TiO_2$ ratio in Cpx vs. Cpx Mg#.

*4.2.1. Mineralogy of stratovolcano rocks*

Ol in lavas from the Kamen stratovolcano varies from Forsterite $(Fo)_{60}$ to $Fo_{83}$, and exhibits a unimodal distribution with maximum at $Fo_{77–79}$ (Fig. 4a). Trace elements in Ol vary significantly: NiO ranges from 0.01% to 1.12%, $Cr_2O_3$ from 0.01% to 0.06%, and CaO from 0.1% to 0.28%. The $NiO/Cr_2O_3$ and NiO/CaO ratios are quite low and range from 0.38 to 3.5 (Fig. 5a).

Cpx in stratovolcano rocks are augites with magnesian numbers (Mg# = Mg/(Mg + Fe)) 79 similar to those of Ol (Fig. 4b). Minor elements in Cpx vary significantly: $Cr_2O_3$ ranges from 0.01% to 0.76%, MnO from 0.09% to 0.60%, $Na_2O$ from 0.02% to 0.50%, and $TiO_2$ from 0.25% to 1.07%. $Cr_2O_3$ systematically decreases and $TiO_2$ increases with decreasing Cpx Mg#. MnO and $Na_2O$ change negligibly (Fig. 5b).

Stratovolcano lavas have Pl that are characterised by calcic compositions ($An_{87–93}$). Some samples show a bimodal distribution with modes at $An_{50}$ and $An_{90}$ (Fig. 4c).

Oxides are represented by high-Al spinel (Sp), magnetite, and titaniferous magnetite. Cr spinel was not found.

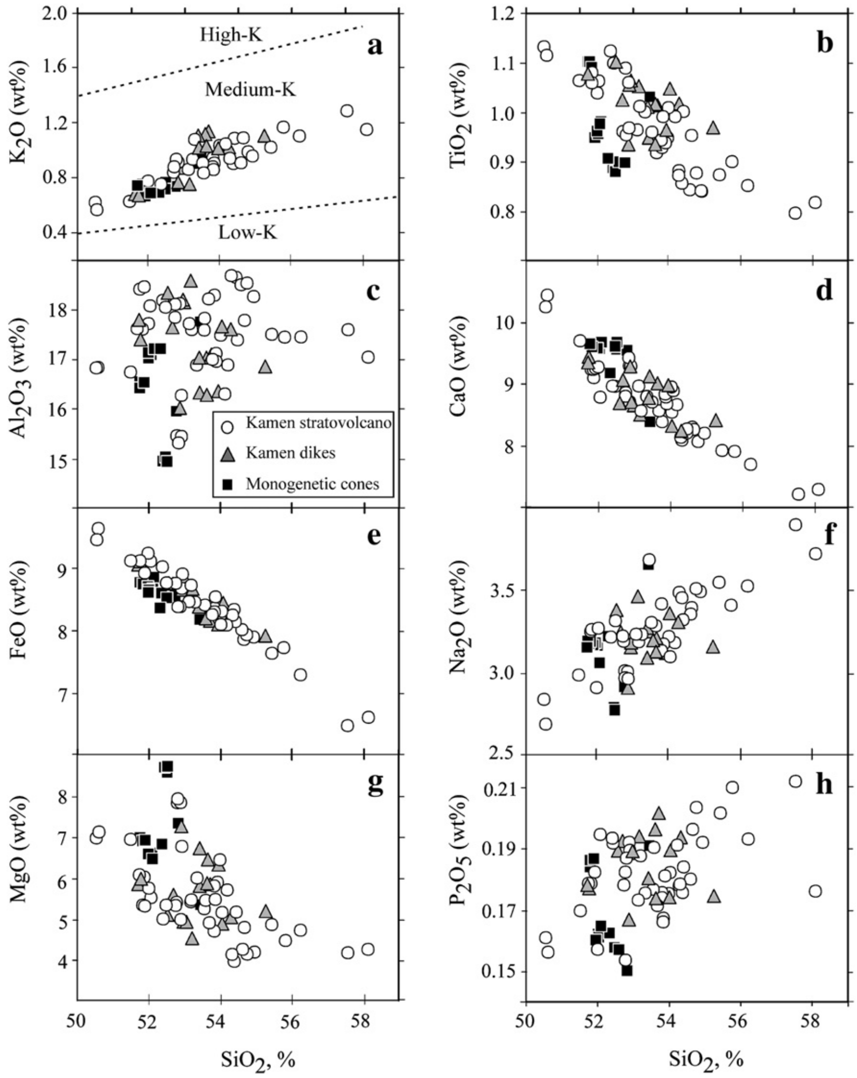


**Fig. 6.** Major elements vs. $SiO_2$ in Kamen Volcano rocks.

*4.2.2. Mineralogy of samples from the dike complex*

Ol from Kamen Volcano dike rocks varies from $Fo_{66}$ to $Fo_{80}$, in the same range as Ol in stratovolcano lavas. The distribution of Ol composition in sample KAM-08-A1 is bimodal with modes at $Fo_{70}$ and $Fo_{78}$ (Fig. 4d). CaO in Ol varies from 0.15% to 0.27%.

Cpx from dikes is again augite with Mg# from 74 to 78, close to the Mg# of Ol from the same rock. The distribution of Cpx Mg# is unimodal with maximum mode at Mg#76 (Fig. 4e). Minor elements in Cpx from the dikes overlap those from stratovolcano samples: MnO from 0.28% to 0.45%, $Na_2O$ from 0.27% to 0.61%, and $TiO_2$ from 0.36% to 1.00%. Like Cpx from the stratovolcano samples $TiO_2$ is negatively correlated with Cpx Mg#, while concentrations of MnO and $Na_2O$ remain constant.

Pl in dike rocks ranges in composition from $An_{78}$ to $An_{88}$ and shows a unimodal distribution with maxima at $An_{84–86}$ (Fig. 4f). Some differences in Pl compositions exist between the stratovolcano lavas and the dike complex: Pl from stratovolcano samples exhibits a bimodal An content distribution, reflecting two stages of Pl crystallization. However, low-An Pl was absent from the dike samples probably due to faster cooling and less extensive crystallization of dike rocks compared to lava flows from the stratovolcano.

*4.2.3. Mineralogy of monogenetic cone lavas*

Ol from monogenetic cones varies from $Fo_{70}$ to $Fo_{92}$ with a unimodal distribution and a maximum at $Fo_{88}$ (Fig. 4g). Minor elements in Ol from two samples are very similar: NiO concentrations range from 0.35% to 0.6% and CaO from 0.15% to 0.35%.

The Mg# of Cpx from monogenetic cones is significantly lower than that of Ol from the same rock and varies from 72 to 80 with a maximum at Mg# = 79 (Fig. 4h). MnO varies from 0.24% to 0.46%, $Na_2O$ from 0.21% to 1.08%, and $TiO_2$ from 0.27% to 0.75%. Pl exhibits a unimodal distribution ($An_{55–75}$) and a maximum at $An_{65}$.

*4.3. Major and trace elements in Kamen rocks*

*4.3.1. Major elements*

The rocks of all three Kamen Volcano units – stratovolcano, dikes, and monogenetic cones – belong to a medium-K calc-alkaline basalt–basaltic–andesitic series (Fig. 6). In detail, however, there are some differences in the trends for major and trace elements. Rocks from the stratovolcano are high-Al, low-Mg basalts and andesites (MgO ≤ 7%, $SiO_2$ ~ 50 to 56%) and form common trends on all variation diagrams with increasing $K_2O$ (Fig. 6a) and decreasing $Al_2O_3$, $TiO_2$, CaO, FeO, and MgO from basalts to andesites (Fig. 6b–d, g). At the same time $Na_2O$ and $P_2O_5$ (Fig. 6f, h) are almost constant. The range of $SiO_2$ in stratovolcano rocks is larger than in other Kamen Volcano units. Ol-free andesites with $SiO_2$ = 55% to 58% were found only in the stratovolcano sequence. Samples from the dike complex fall into the same compositional range of the stratovolcano field (Fig. 6). It is

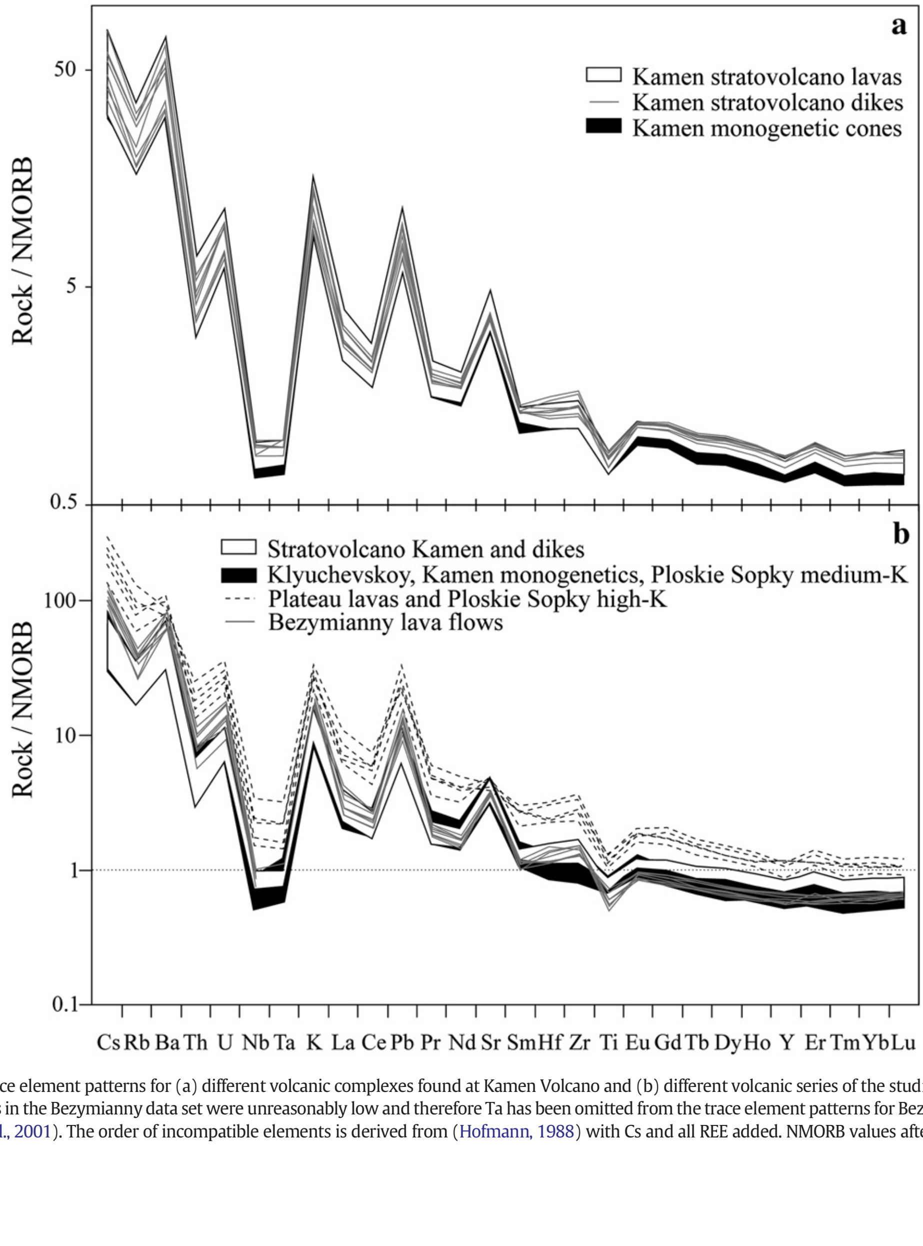


**Fig. 7.** NMORB-normalized trace element patterns for (a) different volcanic complexes found at Kamen Volcano and (b) different volcanic series of the studied Klyuchevskaya group of volcanoes (KGV). The Nb/Ta ratios in the Bezymianny data set were unreasonably low and therefore Ta has been omitted from the trace element patterns for Bezymianny. Data for KGV are from (Almeev, 2005; Churikova et al., 2001). The order of incompatible elements is derived from (Hofmann, 1988) with Cs and all REE added. NMORB values after (Sun and McDonough, 1989).

therefore reasonable to assume that these dikes may be the feeders to, and have a genetic relationship with the lavas.

Monogenetic cone lavas are systematically different from both Kamen stratovolcano lavas and dikes. These isolated cones are all basalts (>6% MgO, 50.5–52.5% $SiO_2$), many are rich in Ol (Table 2), and they exhibit the most magnesian compositions found at Kamen Volcano. Their mineral compositions also differ from those of the stratovolcano samples. In terms of major element composition, monogenetic cones are higher in MgO and CaO and lower in FeO, $TiO_2$, $Al_2O_3$, and $P_2O_5$ at similar $SiO_2$ contents than are stratovolcano and dike rocks. On major element diagrams monogenetic cones form separate trends (Fig. 6b, c, f, h) or fields (Fig. 6d, e, g), which often do not overlap with the stratovolcano samples.

*4.3.2. Trace elements*

Trace element patterns for different Kamen Volcano lava suites are shown in Fig. 7a. All rocks have typical arc signatures with strong but variable large ion lithophile element (LILE) and light rare earth element (LREE) enrichment and low high field strength element (HFSE) concentration. All Kamen Volcano rocks are depleted in Nb and Ta and REE compared to normal mid-ocean ridge basalt (NMORB). In detail, however, there are two main signatures. First, the stratovolcano and dike samples overlap in their trace element patterns (Fig. 7). They also form similar fields and trends on all binary trace element diagrams. In contrast, monogenetic cone rocks are much lower in REE, Nb, and Ta, and fall into separate fields and trends on binary trace element and trace element ratio diagrams (Fig. 6).

## 5. Interpretation

*5.1. Differences and variability of lavas from the Klyuchevskaya group of volcanoes*

Our data from Kamen Volcano lavas show that major and trace elements as well as the mineral compositions of rocks from the stratovolcano and dikes are similar. This suggests that both suites crystallized from the same parental melts under comparable pressure–temperature (P–T) conditions and were derived from similar mantle sources. Similar Ol and Cpx Mg# in stratovolcano and dike rocks also suggest that both minerals are in equilibrium, but they do not fall on the mantle array (Ozawa, 1984). Low $Ol_{Mg\#}$ and $Cpx_{Mg\#}$ and low Ni and Cr concentrations in both minerals show that these magmas were significantly fractionated and do not represent primary melt compositions. This conclusion is confirmed by the absence of high-Cr Sp inclusions in Ol.

At the same time systematic differences in rock and mineral composition exist between Kamen stratovolcano/dikes and monogenetic cones, which simply reflect the different degrees of differentiation of these suites. Most Ol from the more mafic monogenetic basaltic andesite cones are $>Fo_{85}$, whereas Ol from more differentiated stratovolcano lavas are $<Fo_{85}$. Cpx in monogenetic samples is also more

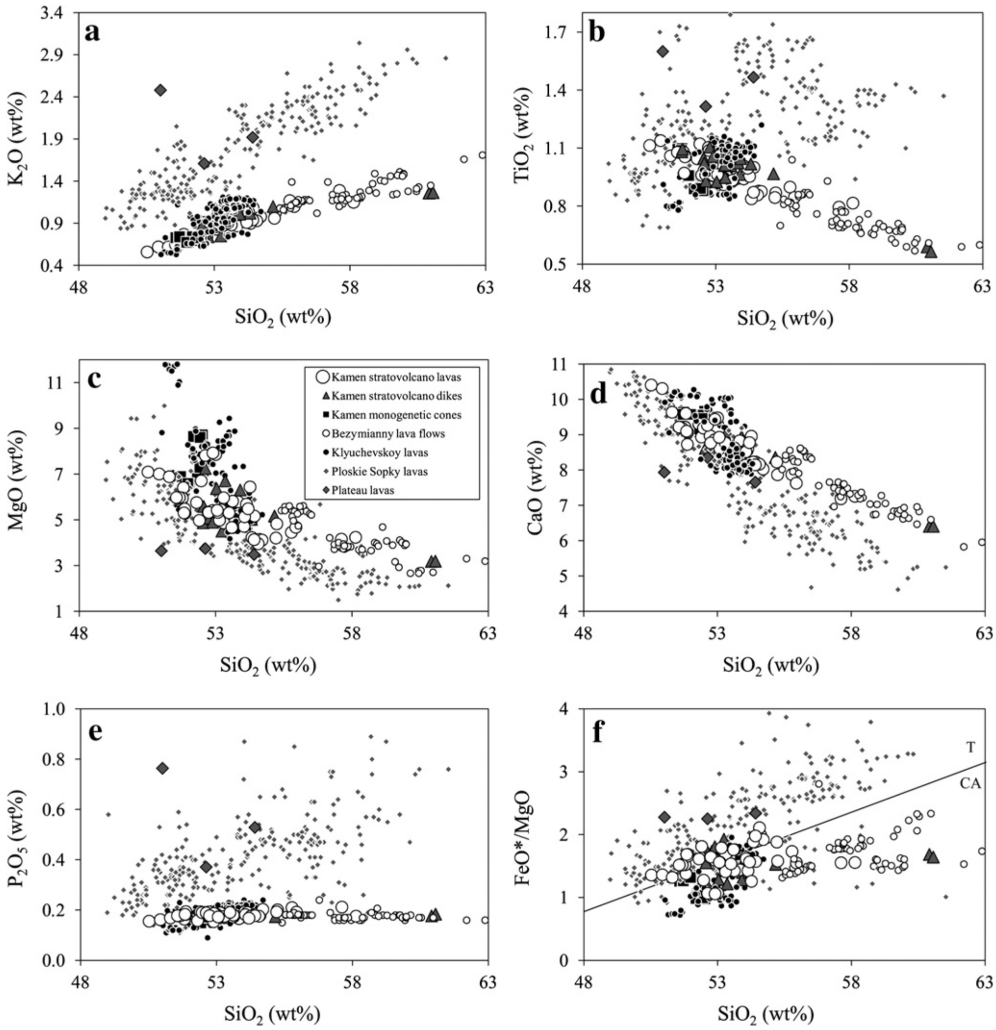


**Fig. 8.** Major elements (a–e) and $FeO^*/MgO$ (f) vs. $SiO_2$ in rocks from Kamen Volcano and neighbouring volcanoes. Data for Ploskie Sopky rocks, Bezymianny lava flows, and Klyuchevskoy basaltic andesites are from (Churikova, 1993; Kersting and Arculus, 1994; Ozerov et al., 1997; Pineau et al., 1999; Churikova et al., 2001; Ishikawa et al., 2001; Dosseto et al., 2003; Bindeman et al., 2004; Almeev, 2005; Portnyagin et al., 2007; Turner et al., 2007).

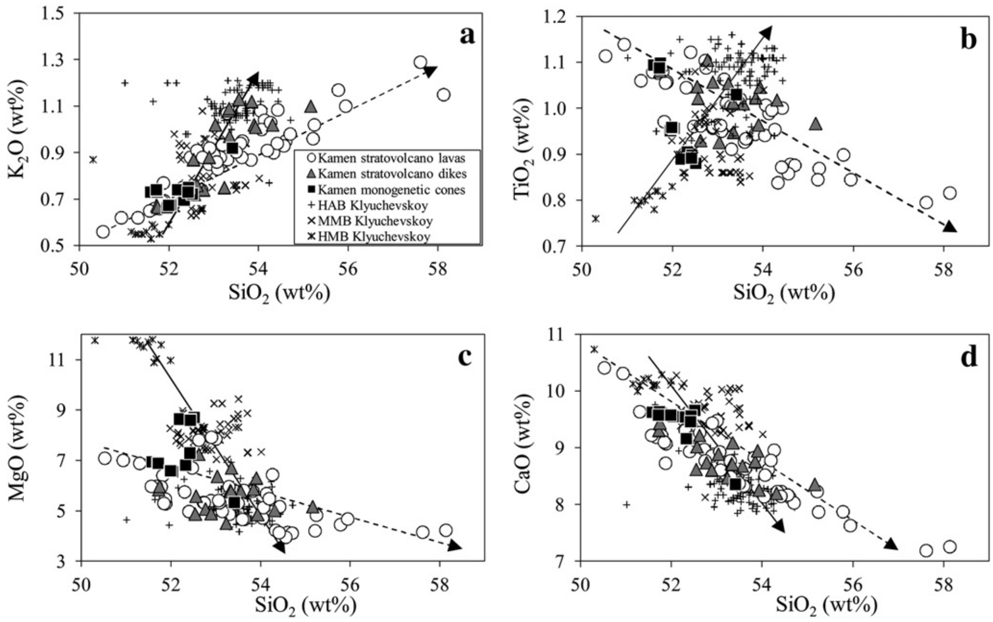


**Fig. 9.** Major elements vs. $SiO_2$ found in Kamen and Klyuchevskoy volcanic rocks. Data for Klyuchevskoy Volcano are from (Portnyagin et al., 2007). HAB — high-aluminium basalts; MMB — moderate-magnesium basalts; HMB — high-magnesium basalts. The black arrow indicates the evolutionary path of Klyuchevskoy melts; the dotted arrow shows the evolutionary path of the Kamen lavas.

magnesian than Cpx in Kamen stratovolcano/dikes. Pl compositions fall between the two Pl generations found in stratovolcano rocks: monogenetic cone Pl compositions are $An_{60-75}$ while stratovolcano and dike Pl compositions are $An_{40-55}$ and $An_{75-90}$.

Mineral assemblages in monogenetic cone rocks are very similar to those documented in Klyuchevskoy Volcano rocks (e.g. Mironov, 2009). In contrast to samples from the stratovolcano and dikes, monogenetic cone Ol is more Mg-rich than is Cpx, suggesting that Cpx crystallized significantly later than Ol and that these minerals were not in equilibrium.

Kamen rocks exhibit major and trace element compositional trends that are distinct from those of Klyuchevskoy and Ploskie Sopky volcanoes but overlap with, and extend the mafic range of lavas from Bezymianny (Figs. 8, 9). Kamen rocks are also distinct from Klyuchevskoy and Ploskie Sopky rocks with respect to the CaO–Fo systematics in their Ol. Again, Ol from Bezymianny lavas falls on an extension of the Kamen Ol trend (Fig. 10). It was shown (Almeev, 2005) that Bezymianny Volcano lavas are compositionally controlled by isobaric crystallization. Because Kamen rocks exhibit the same trend this suggests that the whole Kamen–Bezymianny trend is dominated by fractional crystallization.

Two more observations argue for a close genetic relationship between Kamen and Bezymianny magmas: (1) the occurrence of late-stage Hbl-rich lavas in the evolution of Kamen stratovolcano lavas and dike samples. Compositionally similar Hbl-rich rocks were also erupted at Bezymianny Volcano; and (2) the termination of Kamen Volcano activity 10–11 ka (Melekestsev and Braitseva, 1988), which overlaps directly with the initiation of magmatism at Bezymianny about 10–11 ka ago (Braitseva et al., 1991) (Fig. 3).

Based on MgO and $Al_2O_3$ contents, Klyuchevskoy Volcano rocks can be divided into three groups (e.g. Khrenov et al., 1991; Mironov, 2009): high-Mg basalts (HMB), moderate-Mg basalts (MMB), and high-Al basalts (HAB). These three magma suites are not genetically related by simple low-pressure fractionation. Rather, these magmas either (a) represent high-P fractionated melts from a common arc basalt (Ariskin, 1999), or (b) are derived from the same mantle source with different degrees of melting and magma mixing (Portnyagin et al., 2007), or (c) are derived from distinct sources in the mantle wedge (Kersting and Arculus, 1994).

Klyuchevskoy rocks form a compositional field generally distinct from the Kamen–Bezymianny trend (Figs. 9, 11) at $SiO_2 = 53\%–54\%$, in the field of Klyuchevskoy HAB lavas (Fig. 9). MgO in Klyuchevskoy rocks decreases strongly from 12% to 3.5% over a small range of $SiO_2$ (51% to 54.5%). In contrast, in Kamen Volcano lavas MgO decreases from 7% to 3.5% over an $SiO_2$ range from 50% to 56% (Fig. 9c). The $TiO_2$ distribution is also distinct in the two volcanic series: in Klyuchevskoy samples, $TiO_2$ shows a positive, and Kamen Volcano rocks a negative correlation with $SiO_2$ (Fig. 9b).

Even though Ol (Fig. 4a, m) and Cpx (Fig. 4b, n) in both series are quite similar in major elements, they are systematically different in trace elements: Kamen stratovolcano Ol exhibits a low NiO/CaO ratio compared to Klyuchevskoy HAB lava Ol (Fig. 5a). Kamen stratovolcano lava Cpx exhibits a 2–3 times lower $Na_2O/TiO_2$ ratio than Cpx in HAB rocks from Klyuchevskoy (Fig. 5b). Moreover, Pl compositions are also very different: Kamen stratovolcano Pl shows two separate generations with $An_{50-60}$ and $An_{80-90}$, while Pl from Klyuchevskoy HAB falls exactly in between the two types at $An_{60-70}$.

Samples similar to Klyuchevskoy HMB were not found at Kamen Volcano. However, Kamen monogenetic cone lavas are close to the Klyuchevskoy MMB field on all major and trace element diagrams

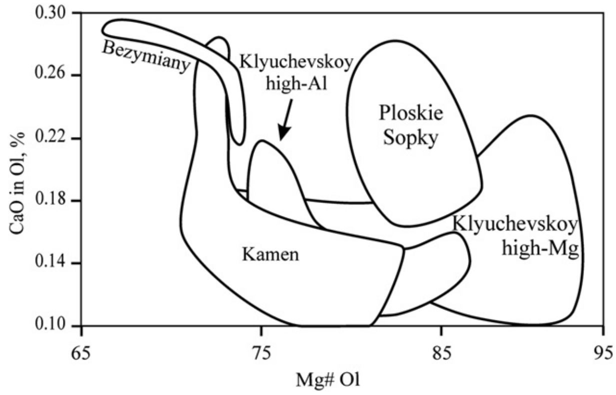


**Fig. 10.** CaO vs. Mg# in Ol for Klyuchevskaya group of volcanoes rocks. There is a trend from Klyuchevskoy through Kamen to Bezymianny volcanoes. Ol from the Ploskie Sopky Volcano form a field that is separate from this trend.

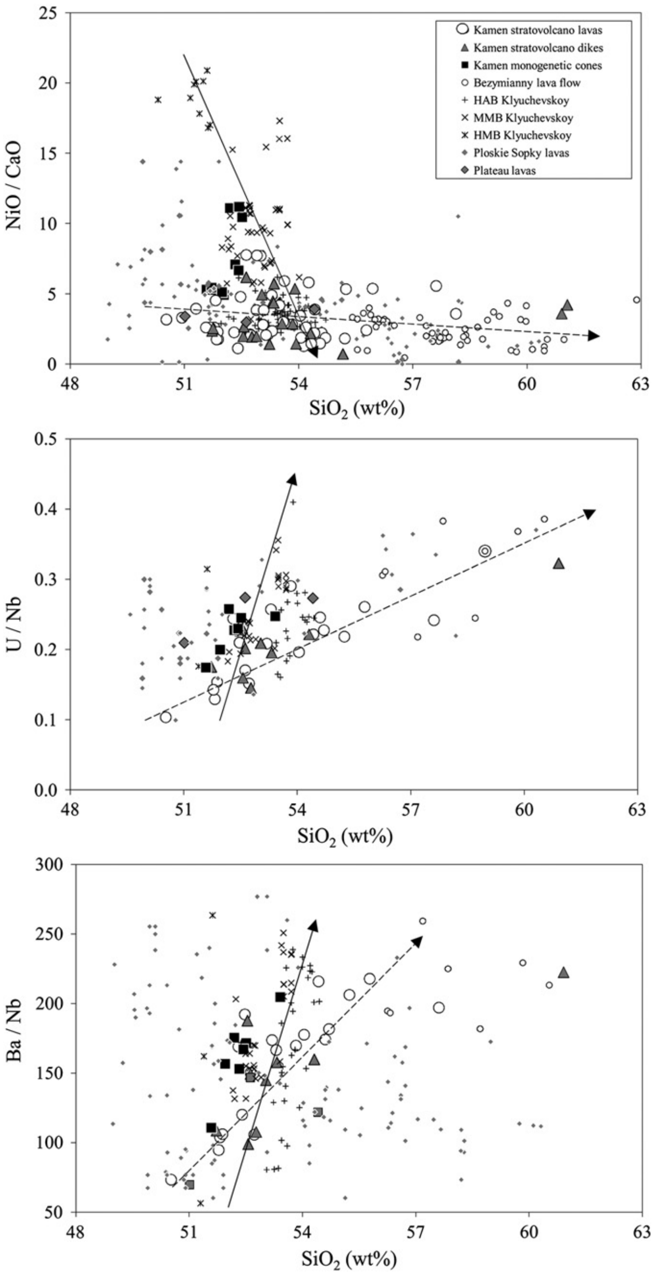


**Fig. 11.** Trace element ratios vs. $SiO_2$ in studied Klyuchevskaya group of volcanoes rocks. The black arrow shows the evolutionary path of the Klyuchevskoy melts; the dotted arrow indicates the evolutionary path of the Kamen–Bezymianny lavas. HAB — high-aluminium basalts; MMB — moderate-magnesium basalts; HMB — high-magnesium basalts.

and in mineral compositions (Fig. 4g–h, p–q), suggesting their genetic relationship.

From these observations, a direct genetic relationship is suggested between Klyuchevskoy MMB and monogenetic cones from Kamen, implying the same primary melts and mantle sources for these two volcanic series. These new data confirm an earlier suggestion based on field work (I.V. Melekestsev, A.P. Maksimov, pers. com.) and our own observations of the morphologies and ages of these cones: (1) they are situated on the slopes of Kamen Volcano and were active after Kamen Volcano activity had ended (i.e. after a series of gravitational collapses); (2) most of the Klyuchevskoy Volcano cinder and cinder–lava cones are situated at some distance (between 7 and 15 km) from the centre of the main edifice (see Fig. 1 in Ozerov et al., 1997) and thus overlap with the monogenetic cinder cones around Kamen, at a distance of 9 to 14 km from Klyuchevskoy; (3) the age of the studied cones is about 2–3.5 ka BP (unpublished data from O.A. Braitseva and V.V. Ponomareva), being a much later occurrence relative Kamen Volcano's ceased activity (Melekestsev and Braitseva, 1988) but coeval with the evolution of Klyuchevskoy (Fig. 3).

The rocks of Ploskie Sopky Volcano, the oldest of the KGV, form systematically different trends from all studied KGV on major and trace element diagrams and thus cannot have originated from the same magma source by fractional crystallization. They are enriched in $K_2O$, $TiO_2$, and $P_2O_5$ and depleted in MgO and CaO (Fig. 8). Ol from Ploskie Sopky Volcano is also highly enriched in CaO compared to Ol from all other KGV volcanoes studied (Fig. 10). Three samples of plateau lavas, which are older still, overlap with the Ploskie Sopky compositional field.

### *5.2. The evolution of the mantle wedge below KGV*

Fig. 7b shows the trace element patterns of rocks from Kamen, compared to other KGV and older plateau lavas. HFSE and HREE are assumed to have low concentrations in the slab fluid (Brenan et al., 1995; Ayers et al., 1997; Stalder et al., 1998). Thus for these elements the mantle contribution is much greater than the slab contribution. From the HFSE and HREE we approximate the patterns of a melt derived from a mantle source without slab-fluid enrichment for plateau lavas and Kamen and Klyuchevskoy stratovolcanoes. These three rock suites have very similar patterns of fluid-immobile trace elements; only the absolute abundances differ, with higher concentrations in the older plateau lavas compared to the younger studied KGV. Also, the degree of slab-fluid enrichment appears to be different: Nb–Ta concentrations relative to elements such as La or Ba in these older rocks (i.e. ratios of HFSE/LILE) are somewhat lower than in younger KGV lavas. Plateau magmas are also enriched in $Na_2O$, $TiO_2$, and $P_2O_5$ and are characterised by higher Nb/Yb and La/Yb but lower Ba/Nb and Ba/La ratios. The ratios of middle to heavy REE in older plateau basalts are close to unity. This suggests that the mantle wedge was less depleted and close in composition to NMORB mantle during the formation of the voluminous plateau lavas around 260–270 ka.

In contrast, most Holocene and historical lavas of the Klyuchevskoy and Ploskie Sopky volcanoes were formed from a more depleted mantle source, which is shown by lower Nb, Ta, and HREE. $HREE_{Klyuch}/HREE_{NMORB}$ varies from 0.52 to 0.55. Monogenetic cone rocks from the western Kamen Volcano slope exhibit the same depleted characteristics. Since we can assume similar and relatively large degrees of melting (10–12% (Churikova et al., 2001)), the fluid-immobile incompatible elements in the mantle wedge became successively depleted with time. Only the younger lavas of the High-K series Ploskie Sopky Volcano rocks were also derived from less-depleted subduction-modified MORB mantle.

We relate this depletion to the massive melting event that formed the voluminous plateau lavas. Further depletion is related to subsequent stratovolcano formation. For example, lavas that erupted from Kamen Volcano at the end of volcanic activity in the early Holocene (around 10 to 11 ka; Melekestsev and Braitseva, 1988) are more depleted in HREE and other non-fluid-mobile elements than plateau lavas, but enriched compared to the younger HMB and MMB from Klyuchevskoy and Moderate-K series rocks from Ploskie Sopky.

### *5.3. Differences in fluid composition*

All studied KGV rocks have typical arc signatures similar to other Kamchatka arc rocks with strong but variable LILE and LREE enrichment of fluid-mobile elements (Cs, Rb, Ba, U, Pb, Sr, K) and a negative Nb–Ta anomaly (Fig. 7b, Dorendorf et al., 2000; Churikova et al., 2001).

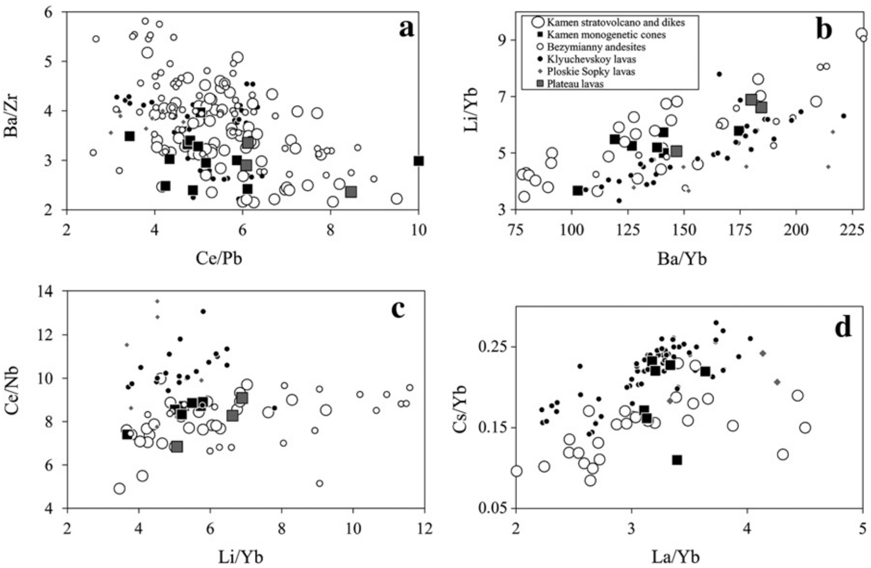


**Fig. 12.** The behaviour of the fluid-mobile/fluid-immobile trace element ratios in Kamen and Klyuchevskoy volcanic rocks. The differing fluid compositions can be seen in both series.

The ratios of the fluid-mobile to fluid-immobile trace elements in Kamen Volcano rocks and in other studied KGV lavas are shown in Fig. 12.

Low Ce/Pb ratios reflect fluid enrichment, because Pb is highly mobile in slab fluids but behaves similar to Ce in the melting and crystallization processes (Miller et al., 1994). Results from earlier work, however, indicate no systematic change in that ratio depending upon the depth of the slab surface across the Kamchatka arc (Churikova et al., 2001). This ratio also does not change significantly in KGV rocks (Fig. 12a). Other ratios that are commonly used to characterise different fluid signatures such as $K_2O$/Rb, Ba/Zr, and Ba/La are also more or less constant in KGV samples. This suggests largely similar fluid signatures in all KGV magmas. This observation can be explained by (1) the same amount of the same fluid or (2) different amounts of fluids with variable trace element content but similar trace element pattern.

Despite the fact that most trace element ratios are rather similar in all KGV rocks, some fluid-mobile/immobile trace element ratios show variations between different volcanic suites. For example, Klyuchevskoy Volcano rocks are systematically enriched in Cs/Yb, and Kamen Volcano lavas are enriched in Li/Yb (Fig. 12).

Ol melt inclusion studies across the Kamchatka arc (Churikova et al., 2007) have shown that the fluid composition changes only gradually with increasing slab depth. Moreover, three different fluids were distinguished from arc front to back arc: (1) B-rich frontal fluid which carries the highest amounts of B, Cl, and chalcophile elements as well as LILE (U, Th, Ba, Pb), F, S, and LREE (La, Ce); (2) CKD fluid enriched in S, U, $^{87}$Sr, and $^{18}$O, and (3) Li-rich back arc fluid with enrichment in F, Li, Be, LILE, and LREE. This fluid variety has been attributed to the dehydration of water-rich minerals at different depths (Schmidt and Poli, 1998).

Comparing the observed fluid signatures across the arc (Churikova et al., 2007) with lavas from the KGV we find that the same three fluids are involved in KGV magma genesis: (1) the B-rich "frontal" arc fluid, that was transported its maximum distance to the depth of magma formation below the volcanic front and is related to a relatively cold subducted slab, (2) the "central" fluid that dominates below the KGV where rifting and decompression is combined with flux-melting of a deeper source, and (3) the influence of the "back arc" fluid, which dominates the magmas erupted at Sredinny Range and contributes to the KGV magma source.

Differences are observed between the Kamen and Klyuchevskoy B/Yb, F/Yb, and Li/Yb ratios (Fig. 13). Klyuchevskoy compositions show good correlations of F/Yb with B/Yb (Fig. 13a), but not with Li/Yb (Fig. 13b), suggesting the influence of "frontal" and "central" fluids. Samples from Kamen Volcano are enriched in all three ratios resulting in positive correlation between them and suggesting the influence of all three fluids. The Cl/S ratio in Kamen melts is 2–3 times higher than in Klyuchevskoy melts (Churikova et al., 2007). These data testify to the different fluid compositions added to the mantle sources of Kamen and Klyuchevskoy volcanoes.

Thus, the distribution of trace and volatile elements in KGV rocks and melt inclusions shows that the fluid composition can differ between neighbouring volcanoes. The KGV appear to be a place where

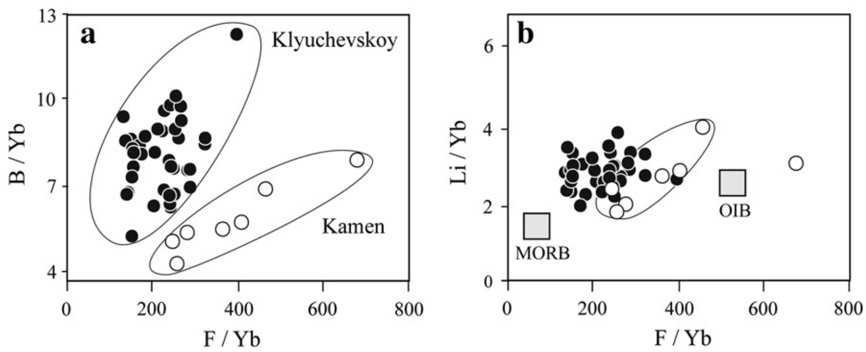


**Fig. 13.** B–Li–F systematics in Kamen and Klyuchevskoy Ol melt inclusions. Data are from (Churikova et al., 2007). MORB — mid-ocean ridge basalt; OIB — ocean island basalt.

**Table 3**
Representative mineral composition analyses of Kamen Volcano rocks.

Olivines

| Complex | Sample | $SiO_2$ | $TiO_2$ | $Al_2O_3$ | FeO | MgO | MnO | CaO | NiO | $Cr_2O_3$ | Total |
|---|---|---|---|---|---|---|---|---|---|---|---|
| Stratovolcano | 2310 | 37.51 | 0.01 | 0.01 | 29.75 | 33.19 | 0.54 | 0.20 | 0.04 | 0.02 | 101.27 |
| | 2310 | 38.22 | 0.05 | 0.03 | 24.99 | 37.47 | 0.42 | 0.15 | 0.04 | 0.00 | 101.37 |
| | 2310 | 38.50 | 0.03 | 0.01 | 22.81 | 39.22 | 0.39 | 0.13 | 0.03 | 0.03 | 101.15 |
| | 2310 | 39.29 | 0.02 | 0.01 | 19.86 | 41.66 | 0.29 | 0.12 | 0.08 | 0.05 | 101.38 |
| | 2310 | 39.73 | 0.01 | 0.05 | 16.43 | 44.17 | 0.25 | 0.15 | 0.10 | 0.03 | 100.91 |
| | KAM-08-07 | 37.96 | 0.00 | 0.00 | 27.61 | 34.51 | 0.29 | 0.19 | 0.00 | 0.00 | 100.55 |
| | KAM-08-07 | 37.28 | 0.00 | 0.00 | 24.69 | 36.53 | 0.44 | 0.17 | 0.00 | 0.00 | 99.12 |
| | KAM-08-07 | 37.66 | 0.00 | 0.20 | 22.67 | 37.71 | 0.25 | 0.21 | 0.00 | 0.00 | 98.70 |
| | KAM-08-07 | 38.14 | 0.00 | 0.00 | 20.73 | 39.64 | 0.25 | 0.20 | 0.48 | 0.00 | 99.44 |
| | KAM-08-07 | 38.53 | 0.00 | 0.00 | 19.75 | 39.62 | 0.40 | 0.00 | 0.00 | 0.00 | 98.30 |
| Dike | KAM-08-A1 | 37.14 | 0.00 | 0.00 | 28.61 | 32.65 | 0.49 | 0.00 | 0.00 | 0.00 | 98.88 |
| | KAM-08-A1 | 39.06 | 0.00 | 0.00 | 19.48 | 41.20 | 0.28 | 0.00 | 0.00 | 0.00 | 100.02 |
| | KAM-08-A1 | 38.56 | 0.00 | 0.00 | 19.99 | 40.36 | 0.24 | 0.22 | 0.00 | 0.00 | 99.36 |
| | KAM-08-A1 | 37.89 | 0.00 | 0.00 | 25.84 | 35.71 | 0.52 | 0.00 | 0.00 | 0.00 | 99.97 |
| | KAM-08-A1 | 38.45 | 0.00 | 0.00 | 20.75 | 39.80 | 0.00 | 0.14 | 0.00 | 0.00 | 99.14 |
| Monogenetic cones | KAM-08-01 | 38.71 | 0.00 | 0.00 | 20.03 | 40.85 | 0.00 | 0.24 | 0.00 | 0.00 | 99.83 |
| | KAM-08-01 | 37.01 | 0.00 | 0.00 | 26.07 | 34.70 | 0.36 | 0.24 | 0.00 | 0.00 | 98.38 |
| | KAM-08-01 | 39.53 | 0.00 | 0.00 | 17.34 | 43.72 | 0.00 | 0.31 | 0.36 | 0.00 | 101.25 |
| | KAM-08-01 | 41.12 | 0.00 | 0.00 | 9.46 | 49.69 | 0.00 | 0.15 | 0.47 | 0.00 | 100.89 |
| | KAM-08-01 | 40.57 | 0.00 | 0.00 | 12.04 | 47.38 | 0.36 | 0.00 | 0.00 | 0.00 | 100.35 |
| | KAM-08-67/1 | 40.61 | 0.00 | 0.00 | 11.67 | 47.49 | 0.00 | 0.18 | 0.46 | 0.00 | 100.42 |
| | KAM-08-67/1 | 38.09 | 0.00 | 0.00 | 21.19 | 39.50 | 0.29 | 0.21 | 0.00 | 0.00 | 99.29 |
| | KAM-08-67/1 | 40.89 | 0.00 | 0.00 | 9.47 | 49.69 | 0.00 | 0.29 | 0.00 | 0.00 | 100.33 |
| | KAM-08-67/1 | 40.26 | 0.00 | 0.00 | 13.15 | 45.93 | 0.00 | 0.19 | 0.40 | 0.00 | 99.93 |
| | KAM-08-67/1 | 39.61 | 0.00 | 0.00 | 15.62 | 43.94 | 0.27 | 0.16 | 0.00 | 0.00 | 99.59 |

Clinopyroxenes

| Complex | Sample | $SiO_2$ | $TiO_2$ | $Al_2O_3$ | FeO | MgO | MnO | CaO | NiO | $Cr_2O_3$ | $Na_2O$ | $K_2O$ | Total |
|---|---|---|---|---|---|---|---|---|---|---|---|---|---|
| Stratovolcano | 2310 | 51.03 | 0.74 | 2.70 | 11.43 | 15.11 | 0.37 | 17.73 | 0.00 | 0.01 | 0.40 | 0.00 | 99.5 |
| | 2310 | 49.71 | 0.91 | 4.52 | 8.69 | 14.97 | 0.24 | 20.44 | 0.02 | 0.03 | 0.34 | 0.02 | 99.9 |
| | 2310 | 50.62 | 0.54 | 4.80 | 6.88 | 15.35 | 0.17 | 21.04 | 0.01 | 0.25 | 0.39 | 0.02 | 100.1 |
| | 2310 | 51.33 | 0.55 | 3.47 | 6.00 | 16.14 | 0.14 | 21.89 | 0.04 | 0.45 | 0.21 | 0.03 | 100.2 |
| | 2310 | 52.26 | 0.30 | 2.78 | 5.19 | 16.94 | 0.15 | 21.15 | 0.02 | 0.70 | 0.33 | 0.00 | 99.8 |
| | KAM-08-07 | 49.07 | 0.72 | 5.13 | 9.56 | 12.78 | 0.32 | 21.10 | н.о. | 0.00 | 0.47 | 0.00 | 99.2 |
| | KAM-08-07 | 49.09 | 0.71 | 5.75 | 8.90 | 14.43 | 0.35 | 19.05 | н.о. | 0.00 | 0.94 | 0.00 | 99.2 |
| | KAM-08-07 | 50.57 | 0.72 | 4.12 | 7.74 | 15.06 | 0.00 | 21.57 | н.о. | 0.27 | 0.29 | 0.00 | 100.3 |
| | KAM-08-07 | 49.28 | 0.55 | 5.15 | 6.98 | 15.21 | 0.00 | 20.02 | н.о. | 0.47 | 0.60 | 0.00 | 98.3 |
| | KAM-08-07 | 51.26 | 0.31 | 3.57 | 6.23 | 16.23 | 0.00 | 21.11 | н.о. | 0.28 | 0.45 | 0.00 | 99.4 |
| Dike | KAM-08-A1 | 48.33 | 0.90 | 6.61 | 9.36 | 13.58 | 0.28 | 20.08 | н.о. | 0.00 | 0.47 | 0.00 | 99.6 |
| | KAM-08-A1 | 50.00 | 0.81 | 5.27 | 9.53 | 15.10 | 0.00 | 19.11 | н.о. | 0.00 | 0.61 | 0.00 | 100.4 |
| | KAM-08-A1 | 50.68 | 0.58 | 3.18 | 9.14 | 15.39 | 0.35 | 20.24 | н.о. | 0.00 | 0.45 | 0.00 | 100.0 |
| | KAM-08-A1 | 50.78 | 0.53 | 4.49 | 8.34 | 15.49 | 0.00 | 20.13 | н.о. | 0.00 | 0.39 | 0.00 | 100.1 |
| | KAM-08-A1 | 49.20 | 0.83 | 5.61 | 7.66 | 14.74 | 0.00 | 21.08 | н.о. | 0.00 | 0.42 | 0.00 | 99.5 |
| Monogenetic cones | KAM-08-67/1 | 51.91 | 0.61 | 2.90 | 9.07 | 17.16 | 0.00 | 17.86 | н.о. | 0.39 | 0.28 | 0.00 | 100.2 |
| | KAM-08-67/1 | 52.89 | 0.46 | 2.13 | 8.57 | 18.05 | 0.46 | 17.65 | н.о. | 0.27 | 0.31 | 0.00 | 100.8 |
| | KAM-08-67/1 | 51.94 | 0.29 | 2.20 | 8.36 | 18.17 | 0.24 | 16.97 | н.о. | 0.43 | 0.49 | 0.00 | 99.1 |
| | KAM-08-67/1 | 52.66 | 0.33 | 2.28 | 8.05 | 17.98 | 0.39 | 17.56 | н.о. | 0.67 | 0.36 | 0.00 | 100.3 |
| | KAM-08-67/1 | 52.84 | 0.00 | 2.03 | 7.64 | 17.66 | 0.37 | 18.40 | н.о. | 0.47 | 0.25 | 0.00 | 99.7 |
| | KAM-08-01 | 51.73 | 0.59 | 2.88 | 9.78 | 16.90 | 0.28 | 17.72 | н.о. | 0.00 | 0.41 | 0.00 | 100.3 |
| | KAM-08-01 | 52.83 | 0.53 | 2.10 | 9.26 | 18.34 | 0.32 | 16.86 | н.о. | 0.36 | 0.38 | 0.00 | 101.0 |
| | KAM-08-01 | 52.28 | 0.68 | 2.56 | 8.61 | 17.56 | 0.30 | 17.77 | н.о. | 0.41 | 0.38 | 0.00 | 100.6 |
| | KAM-08-01 | 52.85 | 0.44 | 2.10 | 8.26 | 17.84 | 0.29 | 18.38 | н.о. | 0.32 | 0.36 | 0.00 | 100.9 |
| | KAM-08-01 | 52.38 | 0.51 | 2.53 | 7.70 | 17.70 | 0.00 | 18.13 | н.о. | 0.62 | 0.28 | 0.00 | 99.8 |

Plagioclases

| Complex | Sample | $SiO_2$ | $Al_2O_3$ | FeO | MgO | CaO | $Na_2O$ | $K_2O$ | Total |
|---|---|---|---|---|---|---|---|---|---|
| Stratovolcano | 2310 | 56.38 | 26.18 | 0.84 | 0.09 | 9.31 | 6.09 | 0.43 | 99.5 |
| | 2310 | 54.81 | 27.55 | 0.33 | 0.03 | 10.41 | 5.55 | 0.24 | 99.0 |
| | 2310 | 50.00 | 30.68 | 0.82 | 0.10 | 14.53 | 3.26 | 0.21 | 99.8 |
| | 2310 | 47.01 | 32.51 | 0.73 | 0.06 | 16.65 | 2.04 | 0.08 | 99.1 |
| | 2310 | 45.37 | 33.50 | 0.72 | 0.05 | 17.84 | 1.28 | 0.05 | 98.8 |
| | KAM-08-07 | 47.67 | 31.80 | 0.85 | н.о. | 15.99 | 2.27 | 0.15 | 98.7 |
| | KAM-08-07 | 45.63 | 32.80 | 0.57 | н.о. | 16.80 | 2.02 | 0.15 | 98.0 |
| | KAM-08-07 | 45.50 | 32.78 | 0.65 | н.о. | 17.11 | 1.78 | 0.00 | 97.8 |
| | KAM-08-07 | 46.11 | 33.46 | 0.42 | н.о. | 17.34 | 1.58 | 0.00 | 98.9 |
| | KAM-08-07 | 44.62 | 33.62 | 0.72 | н.о. | 18.05 | 1.28 | 0.00 | 98.3 |
| Dike | KAM-08-A1 | 46.96 | 32.27 | 0.77 | н.о. | 16.06 | 2.38 | 0.00 | 98.4 |
| | KAM-08-A1 | 47.31 | 33.10 | 0.52 | н.о. | 16.96 | 2.21 | 0.00 | 100.1 |
| | KAM-08-A1 | 47.49 | 33.29 | 0.57 | н.о. | 16.87 | 1.99 | 0.00 | 100.2 |
| | KAM-08-A1 | 46.61 | 33.11 | 0.72 | н.о. | 17.32 | 1.78 | 0.00 | 99.5 |
| | KAM-08-A1 | 46.23 | 34.12 | 0.61 | н.о. | 17.75 | 1.46 | 0.00 | 100.2 |

**Table 3** (*continued*)

Plagioclases

| Complex | Sample | $SiO_2$ | $Al_2O_3$ | FeO | MgO | CaO | $Na_2O$ | $K_2O$ | Total |
|---|---|---|---|---|---|---|---|---|---|
| Monogenetic cones | KAM-08-01 | 53.97 | 28.72 | 0.80 | 0.00 | 12.08 | 4.66 | 0.32 | 100.5 |
| | KAM-08-01 | 53.09 | 29.26 | 0.77 | 0.00 | 12.54 | 4.56 | 0.35 | 100.6 |
| | KAM-08-01 | 53.59 | 29.29 | 0.77 | 0.23 | 12.74 | 4.30 | 0.25 | 101.2 |
| | KAM-08-01 | 52.46 | 30.11 | 0.52 | 0.36 | 13.54 | 3.91 | 0.21 | 101.1 |
| | KAM-08-01 | 50.97 | 31.37 | 0.60 | 0.00 | 14.67 | 3.44 | 0.31 | 101.4 |
| | KAM-08-67/1 | 53.44 | 28.47 | 0.89 | 0.23 | 11.57 | 4.33 | 0.29 | 99.2 |
| | KAM-08-67/1 | 52.82 | 29.16 | 0.71 | 0.22 | 12.74 | 4.23 | 0.22 | 100.1 |
| | KAM-08-67/1 | 52.42 | 29.26 | 0.55 | 0.23 | 12.76 | 4.11 | 0.24 | 99.6 |
| | KAM-08-67/1 | 52.20 | 29.27 | 0.60 | 0.21 | 13.00 | 4.00 | 0.14 | 99.4 |
| | KAM-08-67/1 | 51.23 | 29.76 | 0.56 | 0.18 | 13.39 | 3.75 | 0.24 | 99.1 |

Oxides

| Complex | Sample | $SiO_2$ | $TiO_2$ | $Al_2O_3$ | FeO | MgO | MnO | CaO | NiO | $Cr_2O_3$ | Total |
|---|---|---|---|---|---|---|---|---|---|---|---|
| Stratovolcano | 2310 | 0.10 | 11.37 | 9.75 | 67.70 | 4.33 | 0.39 | 0.03 | 0.05 | 1.66 | 95.38 |
| | 2310 | 0.33 | 7.13 | 9.61 | 74.50 | 2.52 | 0.50 | 0.47 | 0.01 | 1.08 | 96.21 |
| | 2310 | 0.36 | 18.55 | 1.24 | 72.37 | 2.16 | 0.50 | 0.37 | 0.00 | 0.08 | 95.63 |
| | 2310 | 0.28 | 2.69 | 18.54 | 67.42 | 8.85 | 0.50 | 0.35 | 0.00 | 0.29 | 98.93 |
| | 2310 | 0.20 | 1.40 | 49.34 | 31.69 | 12.68 | 0.21 | 0.03 | 0.10 | 2.61 | 98.25 |

several fluids interact, suggesting heterogeneity in the fluids that modified the mantle.

### 5.4. Primary magma compositions

Ariskin (Ariskin, 1999) used a polybaric version of COMAGMAT-3.0 software to model the development of Klyuchevskoy HAB from HMB parental magmas assuming isobaric crystallization at a variety of pressures from 19 to 7 kbar at temperatures from 1350 to 1110 °C and with 2 wt.% of $H_2O$ in the initial melt. With this polybaric fractionation model about 40% of Ol–Cpx–Sp ± Opx assemblages must be fractionated during ascent of the parental HMB magma, which is in accordance with natural mineral and rock compositions. Almeev (Almeev, 2005) suggested a close relationship between Klyuchevskoy and Bezymianny volcanoes but found that Bezymianny Volcano parental melts do not correspond to Klyuchevskoy HAB which are less primitive (more $SiO_2$ and alkalis, less CaO, Tables 3, 4). For the calculations he used the Bezymianny Volcano andesitic basalt (column 1 in Table 4) which is similar to the Kamen andesitic basalt defined from the present study (column 2 in Table 4). Moreover, our data show that the basalts of Kamen Volcano are even more primitive ($SiO_2$ = 50.5%, MgO = 7%, column 3 in Table 4) than the parental Bezymianny Volcano basaltic andesite ($SiO_2$ = 53.16%, MgO = 5.47%) (Almeev, 2005), continuing the Kamen–Bezymianny trend to more mafic compositions.

Similar trace element distributions and trace element ratios in Klyuchevskoy and Kamen volcanoes suggest that primary melts for both were also similar and that they originated from the same mantle source. However, the Kamen–Bezymianny trend cannot be calculated from Klyuchevskoy lavas by simple low-P fractional crystallization. Also, some differences in whole rock major and trace elements as well as mineral compositions between the two volcanic series are observed.

According to the geochemical trends, Kamen–Bezymianny magmatic system parental melts are HAB-type and MMB-type magmas (Figs. 6, 8, 9). Although comparing different models of high-Al basalt formation is beyond the scope of this paper, it is possible that such melts originated by polybaric fractionation as has been suggested for HMB of Klyuchevskoy (Ariskin, 1999). In this case the Kamen primary melts should have lower amounts of $SiO_2$ and alkalis and higher amounts of CaO compared to the primary Klyuchevskoy melt. However, the absence of high-Mg mafic minerals in Kamen basalts suggests that the formation of Kamen–Bezymianny primary melts occurred at lower P–T conditions than those that prevailed during the formation of Klyuchevskoy HMB.

In summary, our data show an increasingly depleted mantle wedge that is fluxed by slightly different fluids. Magma generation by flux melting combined with decompression melting below the CKD rift produced a series of primary magmas that evolved by polybaric fractionation. Magmatic lineages based on these parent

**Table 4**
Parental melts of studied volcanoes of the Klyuchevskaya group.

| | Parental melt of Bezymianny (Almeev, 2005) | Basaltic andesite of Kamen | Parental melt of Kamen–Bezymianny | Klyuchevskoy primary melt (Ariskin, 1999) | Ploskie Sopky parental melt (Churikova, 1993) |
|---|---|---|---|---|---|
| Sample | Average of 2 | Average of 6 | 2310 | KL-03 | 3–90 |
| $SiO_2$% | 53.16 | 52.82 | 50.76 | 51.82 | 51.03 |
| $TiO_2$% | 1.08 | 1.08 | 1.12 | 0.83 | 0.88 |
| $Al_2O_3$% | 17.90 | 18.14 | 16.90 | 13.34 | 16.08 |
| FeO tot % | 9.15 | 9.05 | 10.04 | 8.85 | 9.55 |
| MnO % | 0.17 | 0.18 | 0.19 | 0.16 | 0.17 |
| MgO% | 5.47 | 5.51 | 7.13 | 11.86 | 7.99 |
| CaO % | 8.89 | 9.08 | 10.46 | 10.27 | 10.45 |
| $Na_2O$% | 3.10 | 3.20 | 2.69 | 2.17 | 2.62 |
| $K_2O$% | 0.92 | 0.76 | 0.56 | 0.58 | 1.01 |
| $P_2O_5$% | 0.18 | 0.18 | 0.16 | 0.12 | 0.22 |
| Sum | 100 | 100 | 100 | 100 | 100 |
| Sc | 30 | 31 | 39 | 35 | 32 |
| V | 282 | 272 | 316 | 236 | 294 |
| Cr | 22 | 41 | 220 | 760 | 312 |
| Ni | 19 | 18 | 33 | 186 | 82 |
| Sr | 302 | 309 | 291.5 | 242 | 450 |
| Ba | 290 | 349 | 180.00 | 202 | 279 |
| La | 5 | 6.59 | 4.58 | 4 | 6.49 |
| Ce | 14 | 14.69 | 12.04 | 10 | 15.0 |
| Pr | 2.3 | 2.36 | 2.03 | 1.6 | 2.29 |
| Nd | 11 | 12.19 | 11.23 | 8 | 12.21 |
| Sm | 3.1 | 3.48 | 3.17 | 2.2 | 3.25 |
| Eu | 1.1 | 1.19 | 1.10 | 0.8 | 0.97 |
| Gd | 3.7 | 4.12 | 3.53 | 2.7 | 3.11 |
| Tb | 0.6 | 0.68 | 0.68 | 0.4 | 0.44 |
| Dy | 4 | 4.51 | 3.87 | 3 | 2.70 |
| Ho | 0.8 | 0.92 | 0.83 | 0.6 | 0.61 |
| Er | 2.3 | 2.79 | 2.39 | 1.6 | 1.64 |
| Tm | 0.4 | 0.38 | 0.35 | 0.2 | 0.22 |
| Yb | 2.4 | 2.59 | 2.29 | 1.6 | 1.57 |
| Lu | 0.4 | 0.38 | 0.35 | 0.2 | 0.25 |
| Hf | 2.3 | 2.6 | 1.92 | 1.6 | 1.59 |
| Ta | 0.2 | 0.11 | 0.14 | 0.1 | 0.07 |
| Tl | 0.08 | 0.05 | 0.05 | 0.05 | 0.06 |
| Pb | 2.9 | 2.24 | 2.19 | 3.4 | 3.20 |
| Th | 0.5 | 0.45 | 0.48 | 0.4 | 0.74 |
| U | 0.3 | 0.37 | 0.25 | 0.2 | 0.33 |

magmas can be attributed to different stratovolcanoes and their surrounding monogenetic centres.

## 6. Conclusions

1) Data on major and trace elements in rocks from Kamen Volcano and neighbouring volcanoes fall into three distinct geochemical groups. Lavas from the Kamen stratovolcano and its dikes are distinct in their geochemical character from magmas erupted at Ploskie Sopky and Klyuchevskoy.
2) A close genetic relationship exists between Kamen and Bezymianny volcanoes in which the Bezymianny lavas comprise the more evolved part of the common trends. This Kamen–Bezymianny trend is dominated by fractional crystallization and magma mixing and is typical for many arc magma series. This trend suggests that Kamen Volcano shares the magma source and a common magma plumbing system with Bezymianny Volcano.
3) Monogenetic cinder and cinder–lava cones situated on the W–SW slopes of Kamen Volcano are compositionally similar and thus genetically related to Klyuchevskoy Volcano (MMB lavas).
4) Klyuchevskoy lavas are geochemically separate from the Kamen–Bezymianny rocks and define three distinct magma compositions that are not genetically related by simple low-pressure fractionation and/or mixing. Rather, these magmas either (a) represent high-P fractionated melts from a common arc basalt, or (b) are derived from the same mantle source with different degrees of melting and magma mixing, or (c) are derived from distinct sources in the mantle wedge.
5) Ploskie Sopky Volcano rocks are systematically different from Kamen and Klyuchevskoy rocks in major elements and mineral composition; some are similar to the older plateau lavas. Thus they could not have originated from the same primary melts by fractional crystallization.
6) The geochemical diversity of KGV rocks and their relationship to underlying plateau lavas results from both (a) gradual depletion with time of the mantle NMORB-type source due to previous magmatic events, and (b) the addition of distinct and variable fluids to this mantle source.
7) Trace and volatile element ratios in rocks and melt inclusions show that the fluid composition can differ even between neighbouring volcanoes with rather similar mantle sources.

Supplementary data to this article can be found online at http://dx.doi.org/10.1016/j.jvolgeores.2013.01.019.

## Acknowledgements

We are very grateful to Benjamin Andrews, Malcolm Rutherford and an anonymous reviewer for their useful comments on an earlier version of the manuscript. The authors thank colleagues from the IViS DVO RAS, participants in the PIRE project funded by NSF, and our volunteers who helped make the challenging field work at Kamen Volcano successful: O.E. Bograd, Yu.V. Demyanchuk, N.P. Egorova, Ya.D. Muraviev, A.Yu. Ozerov, S.V. Ushakov, V.P. Fedulova, V.V. Yaschuk, M.M. Yarin, E.Yu. Boyarskikh, P.E. Izbekov and A.S. Kirilenko. Useful comments by V.V. Ponomareva, A.B. Belousov, M.B. Belousova, Yu.B. Slezin, Ya.D. Muraviev, and discussions with I.V. Melekestsev and A.P. Maksimov helped us to improve this manuscript. We thank A.P. Maksimov for providing us with Pre-Bezymianny Volcano samples. We appreciate Ms. Candace O'Connor's input in editing of our manuscript.We are grateful to Lomonosov MSU students I.A. Lebedev and A.A. Griban for providing us with microprobe data. We are grateful to the Russian Foundation for Basic Research grant § 08-05-00600 for supporting this work.

## References

Almeev, R.R., 2005. Geochemistry of Bezymianny volcano lavas: signatures of the mantle source and magma fractionation processes. PhD thesis. Vernadsky Institute of geochemistry and analytical chemistry RAS, Moscow (in Russian).
Ariskin, A.A., 1999. Phase equilibria modeling in igneous petrology: use of COMAGMAT model for simulating fractionation of ferro-basaltic magmas and the genesis of high-alumina basalt. Journal of Volcanology and Geothermal Research 90, 115–162.
Ayers, J.C., Dittmer, S.K., Layne, G.D., 1997. Partitioning of elements between peridotite and $H_2O$ at 2.0–3.0 GPa and 900–1100 degrees C, and application to models of subduction zone processes. Earth and Planetary Science Letters 150, 381–398.
Bindeman, I.N., Ponomareva, V.V., Bailey, J.C., Valley, J.W., 2004. Volcanic arc of Kamchatka: a province with high-δ18 O magma sources and large-scale 18O/16O depletion of the upper crust. Geochimica et Cosmochimica Acta 68, 841–865.
Braitseva, O.A., Melekestsev, I.V., Bogoyavlenskaya, G.E., Maksimov, A.P., 1991. Bezymyannyi: eruptive history and dynamics. Volcanology and Seismology 12, 165–194.
Braitseva, O.A., Melekestsev, I.V., Ponomareva, V.V., Sulerzhitsky, L.D., 1995. The ages of calderas, large explosive craters and active volcanoes in the Kuril-Kamchatka region, Russia. Bulletin of Volcanology 57, 383–402.
Brenan, J.M., Shaw, H.F., Ryerson, F.J., Phinney, D.L., 1995. Mineral-aqueous fluid partitioning of trace elements at 900 degrees C and 2.0 GPa; constraints on the trace element chemistry of mantle and deep crustal fluids. Geochimica et Cosmochimica Acta 59, 3331–3350.
Calkins, J.A., 2004. $^{40}Ar/^{39}Ar$ geochronology of Khapitsa plateau and Studyonaya river basalts and basaltic andesites in Central Kamchatka Depression, Kamchatka, Russia. In: Gordeev, E.I. (Ed.), Linkages Among Tectonics, Seismicity, Magma Genesis, and Eruption in Volcanic Arcs. IV International Biennial Workshop on Subduction Processes Emphasizing the Japan–Kurile–Kamchatka–Aleutian Arcs. Institute of Volcanology and Seismology FEB RAS, Petropavlovsk-Kamchatsky, pp. 53–54.
Churikova, T.G., 1993. Geochemistry and modeling of the magmatic processes of the Klyuchevskaya group of volcanoes. PhD thesis. Lomonosov Moscow State University, Moscow (in Russian).
Churikova, T., Dorendorf, F., Wörner, G., 2001. Sources and fluids in the mantle wedge below Kamchatka, evidence from across-arc geochemical variation. Journal of Petrology 42, 1567–1593.
Churikova, T., Wörner, G., Mironov, N., Kronz, A., 2007. Volatile (S, Cl and F) and fluid mobile trace element compositions in melt inclusions: implications for variable fluid sources across the Kamchatka arc. Contributions to Mineralogy and Petrology 154, 217–239.
Dorendorf, F., Wiechert, U., Wörner, G., 2000. Hydrated sub-arc mantle: a source for the Kluchevskoy volcano, Kamchatka/Russia. Earth and Planetary Science Letters 175, 69–86.
Dosseto, A., Bourdon, B., Joron, J.-L., Dupre, B., 2003. U–Th–Pa–Ra study of the Kamchatka arc: new constraints on the genesis of arc lavas. Geochimica et Cosmochimica Acta 67, 2857–2877.
Erlich, E.N., Gorshkov, G.S., 1979. Quaternary volcanism and tectonics in Kamchatka. Bulletin Volcanologique, 42. Springer International [for the] International Association of Volcanology and Chemistry of the Earth's Interior (IAVCEI), Heidelberg, International (298 pp.).
Ermakov, V.A., 1977. Formation Dismemberment of the Quaternary Volcanic Rocks. Nedra, Moscow (223 pp. in Russian).
Flerov, G.B., Ovsyannikov, A.A., 1991. Ushkovsky volcano. In: Fedotov, S.A., Masurenkov, Yu.P (Eds.), Active Volcanoes of Kamchatka, 1. Nauka, Moscow, pp. 164–165.
Ginibre, C., Kronz, A., Wörner, G., 2002. High-resolution quantitative imaging of plagioclase composition using accumulated backscattered electron images: new constraints on oscillatory zoning. Contributions to Mineralogy and Petrology 142, 436–448.
Hofmann, A.W., 1988. Chemical differentiation of the Earth; the relationship between mantle, continental crust, and oceanic crust. Earth and Planetary Science Letters 90, 297–314.
Ishikawa, T., Tera, F., Nakazawa, T., 2001. Boron isotope and trace element systematics of the three volcanic zones in the Kamchatka arc. Geochimica et Cosmochimica Acta 65, 4523–4537.
Ivanov, B.V., 2008. Andesites of Kamchatka. Nauka, Moscow (365 pp. (in Russian)).
Kersting, A.B., Arculus, R.J., 1994. Klyuchevskoy Volcano, Kamchatka, Russia: the role of high-fluxed, recharged, tapped and fractionated magma chamber(s) in the genesis of high-$Al_2O_3$ basalt from high-MgO basalt. Journal of Petrology 35, 1–42.
Khrenov, A.P., Dvigalo, V.N., Kirsanov, I.T., Fedotov, S.A., Gorel'chik, V.I., Zharinov, N.A., 1991. Klyuchevskoy volcano. In: Fedotov, S.A., Masurenkov, Yu.P. (Eds.), Active Volcanoes of Kamchatka, 1. Nauka, Moscow, pp. 146–153.
Melekestsev, I.V., 1980. Volcanism and Relief-formation. Nauka, Moscow (212 pp. in Russian).
Melekestsev, I.V., Braitseva, O.A., 1988. Gigantic collapses on volcanoes. Volcanology and Seismology 6, 495–508.
Melekestsev, I.V., Kraevaya, T.S., Braitseva, O.A., 1970. Relief and Deposits of Young Volcanic Regions of Kamchatka. Nauka, Moscow (in Russian).
Melekestsev, I.V., Braitseva, O.A., Erlich, E.N., Kozhemyaka, N.N., 1974. Volcanic mountains and plains. In: Luchitsky, I.V. (Ed.), Kamchatka, Kurile and Commander Islands. Nauka, Moscow, pp. 162–234 (in Russian).
Melekestsev, I.V., Khrenov, A.P., Kozhemyaka, N.N., 1991a. Tectonic position and general description of volcanoes of Northern group and Sredinny range. In: Fedotov, S.A., Masurenkov, Yu.P. (Eds.), Active Volcanoes of Kamchatka, 1. Nauka, Moscow, pp. 79–81.
Melekestsev, I.V., Volynets, O.N., Ermakov, V.A., Kirsanova, T.P., Masurenkov, Yu.P., 1991b. Sheveluch volcano. In: Fedotov, S.A., Masurenkov, Yu.P. (Eds.), Active Volcanoes of Kamchatka, 1. Nauka, Moscow, pp. 98–103.

Miller, D.M., Goldstein, S.L., Langmuir, C.H., 1994. Cerium/lead and lead isotope ratios in arc magmas and the enrichment of lead in the continents. Nature 368, 514–520.
Mironov, N. L., 2009. Origin and evolution of the magmas of Klyuchevskoy volcano, Kamchatka, data of melt inclusion study in olivine. PhD thesis. Vernadsky Institute of geochemistry and analytical chemistry RAS, Moscow (in Russian).
Mironov, N.L., Portnyagin, M.V., Pletchov, P.Yu., Khubunaya, S.A., 2001. Final stages of magma evolution in Klyuchevskoy volcano, Kamchatka: evidence from melt inclusions in minerals of high-alumina basalts. Petrology 9, 46–62.
Ozawa, K., 1984. Olivin-spinel geospeedometry: analysis of diffusion-controlled Mg–$Fe^{2+}$ exchange. Geochimica et Cosmochimica Acta 48, 2597–2611.
Ozerov, A.Y., 2000. The evolution of high-alumina basalts of the Klyuchevskoy volcano, Kamchatka, Russia, based on microprobe analyses of mineral inclusions. Journal of Volcanology and Geothermal Research 95, 65–79.
Ozerov, A.Yu., Ariskin, A.A., Kyle, Ph., Bogoyavlenskaya, G.E., Karpenko, S.F., 1997. Petrological–geochemical model for genetic relationships between basaltic and andesitic magmatism of Klyuchevskoi and Bezymyannyi volcanoes, Kamchatka. Petrology 5, 550–569.
Pineau, F., Semet, M.P., Grassineau, N., Okrugin, V.M., Javoy, M., 1999. The genesis of the stable isotope (O, H) record in arc magmas: the Kamtchatka's case. Chemical Geology 135, 93–124.
Ponomareva, V.V., Melekestsev, I.V., Dirksen, O.V., 2006. Sector collapses and large landslides on Late Pleistocene–Holocene volcanoes in Kamchatka, Russia. Journal of Volcanology and Geothermal Research 158, 117–138.
Portnyagin, M., Bindeman, I., Hoernle, K., Hauff, F., 2007. Geochemistry of primitive lavas of the Central Kamchatka Depression: magma generation at the edge of the Pacific plate. In: Eichelberger, J., Gordeev, E., Izbekov, P., Kasahara, M., Lees, J. (Eds.), Volcanism and Subduction: the Kamchatka RegionGeophysical Monograph 172, 199–239.
Reiche, P., 1937. The toreva-block — a distinctive landslide type. Journal of Geology 45, 538–548.
Schmidt, M.W., Poli, S., 1998. Experimentally based water budgets for dehydrating slabs and consequences for arc magma generation. Earth and Planetary Science Letters 163, 361–379.
Stalder, R., Foley, S.F., Brey, G.P., Horn, I., 1998. Mineral-aqueous fluid partitioning of trace elements at 900 °C–1200 °C and 3.0 GPa to 5.7 GPa: new experimental data for garnet clinopyroxene and rutile and implications for mantle metasomatism. Geochimica et Cosmochimica Acta 62, 1781–1801.
Sun, S.S., McDonough, W.F., 1989. Chemical and isotopic systematics of oceanic basalts; implications for mantle composition and processes. In: Saunders, A.D., Norry, M.J. (Eds.), Magmatism in the Ocean Basins. Geological Society of London, London, pp. 313–345.
Tokarev, P.I., Zobin, V.M., 1970. The peculiarity of the propagation of the seismic waves of the close earthquakes in the Earth's crust and upper mantle in the area of Klyuchevskaya group of volcanoes at Kamchatka. B. Volcanol. Stations, N 4, pp. 17–23 (in Russian).
Turner, S., Sims, K.W.W., Reagan, M., Cook, C., 2007. A $^{210}Pb$–$^{226}Ra$–$^{230}Th$–$^{238}U$ study of Klyuchevskoy and Bezymianny volcanoes, Kamchatka. Geochimica et Cosmochimica Acta 71, 4771–4785.